FILM COOLING EFFECTIVENESS FOR THREE ROW COMPOUND HOLE DESIGN ON FLAT PLATE USING PSP TECHNIQUE

A Thesis

by

MUHAMMAD HASSAN BASHIR

Submitted to the Office of Graduate and Professional Studies of
Texas A&M University
in partial fulfillment of the requirements for the degree of

MASTER OF SCIENCE

Chair of Committee,	Je Chin Han
Committee Members,	Hamn-Ching Chen
	Partha Mukherjee
Head of Department,	Andreas A. Polycarpou

August 2016

Major Subject: Mechanical Engineering

ABSTRACT

A comprehensive study was performed to investigate effects of geometrical and coolant flow parameters for a three row compound hole design over a flat plate. These included β: +45 and -45, in-line and stagger arrangement, hole spacing (4d, 6d and 8d), five blowing ratios (0.5-1.5) and three density ratios (1.0, 1.5, 2.0). The mainstream Reynold's number was kept constant at 285,000 with a turbulence intensity of 6%. Average effectiveness plots and contours were developed using Pressure Sensitive Paint (PSP) technique and cross comparisons were carried out.

The parametric results obtained from experimentation generally agreed with widely accepted trends: the cascade effect of coolant jets for multi hole design increases overall effectiveness especially at large x/d, increasing density ratio increases effectiveness particularly at higher blowing ratio and increasing hole spacing has a detrimental effect on film cooling. However, few of the more interesting observations included: stagger arrangement is not always the most optimum design (β: +45, -45, -45 with staggered 2^{nd} and 3^{rd} row reported the lowest effectiveness for all blowing ratios and density ratios); inline arrangement of holes with opposing orientation angles (β: +45, -45, -45) yields better effectiveness; blowing ratio effect is strongly dependent on geometric design. Moreover, hole spacing effect is closely related to neighboring coolant jet coalescence and interaction with mainstream flow.

Currently, little data is available on three row design in open literature; this study provides systematic, baseline information for future studies.

ACKNOWLEDGEMENTS

I would like to thank my committee chair, Dr. J.C Han, and my committee members, Dr. Chen, and Dr. Mukherjee, for their guidance and support throughout the course of this research.

Thanks also go to my friends and colleagues from Turbine Heat Transfer Lab with special mention of Dr. Li, Joe, Nafiz and Andy for making my time at Turbine Heat Transfer Lab a great experience. I also want to extend my gratitude to the Fulbright Scholarship Program for giving me the opportunity to pursue my MS in United States.

Finally, thanks to my mother and father for their encouragement and prayers.

NOMENCLATURE

α	Axial angle to the mainstream
β	Compound angle to the mainstream
η	Film cooling effectiveness
ρ	Density, kg/m^3
C	Mass fraction
d	Diameter of film cooling hole
DR	Coolant to mainstream density ratio
I	PSP emission intensity
l/d	Injection hole length to diameter ratio
M	Blowing ratio/ Mass flux ratio
MFR	Coolant to mainstream mass flow rate
nps	Nominal pipe size
p/d	Hole spacing to diameter ratio
PIV	Particle image velocimetry
s/d	Row spacing
T	Temperature
Tu	Turbulence intensity

Subscript

∞	Mainstream air property

A_w	Adiabatic wall
blk	Black condition
c	Coolant
f	Film
f_g	Foreign gas (N_2, CO_2, Mixture of SF_6 and Ar)
m	Mainstream
ref	Reference condition
w	Wall

TABLE OF CONTENTS

Page

LIST OF FIGURES

Page

LIST OF TABLES

Page

1. INTRODUCTION

Gas Turbines have a wide spread application in aerospace and power sector. Owing to their significance, researchers are continuously exploring opportunities for optimization and efficiency enhancement. Most obvious choice is to increase rotor inlet temperature; however, this is limited by blade material properties [1]. Hot gases (~1700 K) from combustors impinge directly on the 1st stage rotor blades which have to bear the maximum impact. To maintain mechanical integrity and avoid creep failure, effective cooling mechanisms need to be incorporated. These are broadly divided into external cooling, commonly referred to as film cooling and internal cooling. The latter employs turbulent promoters like ribs and pins, as well as impingement cooling to enhance heat transfer effectiveness. In most high temperature applications, both internal and film cooling together with thermal barrier coatings (TBC) are used to obtain conjugate cooling in the blade [2]. Figure 1 highlights major cooling mechanisms for a gas turbine blade.

1.1 Film Cooling

Over the past three decades, film cooling has been widely accepted as primary cooling mechanism for turbine blades [3]. It is the "introduction of a secondary fluid (coolant or injected fluid) at one or more discrete locations along a surface exposed to a high temperature environment to protect that surface not only in the immediate region of injection but also in the downstream region" (Goldstein [4]). In other words, relatively

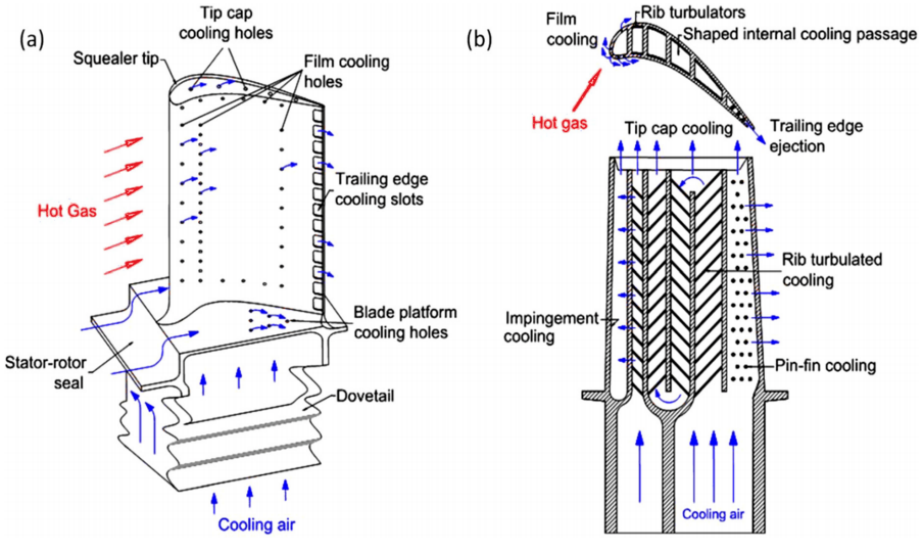

Figure 1: Schematic of blade cooling (a) film cooling (b) internal cooling [1]

cool air is extracted from the axial compressor of gas turbine and ejected through discrete holes present on blade surface forming a protective film – an effective barrier against the incoming hot mainstream gas. Figure 2 describes the film cooling principle for coolant injection from a single hole. Generally, maximum cooling effectiveness is observed immediately next to the hole with a sharp decay moving downstream owing to coolant mixing with the mainstream. To avoid decay, multiple rows of holes are designed into the blade surface.

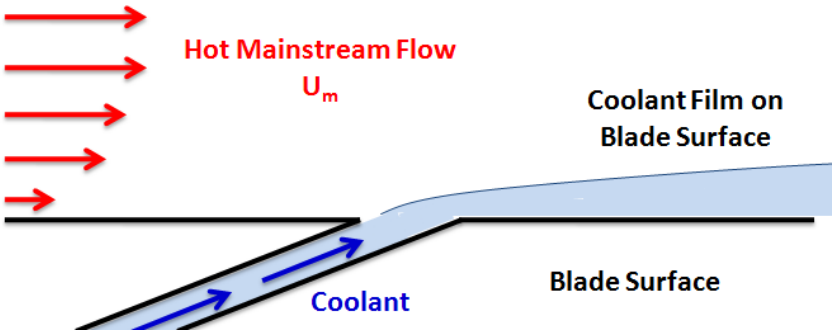

Figure 2: Forward injection film cooling schematic

Coolant air is available only in limited quantities; hence the necessity to accurately predict cooling load and employing the most optimum design. Parameters such a thickness of film, penetration into mainstream and generated turbulence not only impact overall cooling effectiveness, but influence aerodynamic performance of the blade itself.

2. LITERATURE REVIEW

2.1 Flat Plate Film Cooling

For fundamental experimental heat transfer studies on blades, it is a common practice to divide the blade into two parts: leading edge modeled as semi-cylinder and downstream portion approximated as a flat plate. Numerous studies in open literature have employed flat plate to study basic film cooling parameters such a mainstream turbulence, coolant density, hole geometry, surface curvature, surface roughness etc. a review of which can be found in [5-9]. Bogard et al. [7] classifies these parameters into three broad categories: airfoil geometry, hole geometry (stream-wise angle (α), compound angle (β), pitch, row spacing etc.), and coolant / mainstream conditions (turbulence, blowing ratio, density ratio etc.). The scope of current study; however, focuses on the latter two for a three row compound hole design on a flat plate.

2.2 Coolant Hole Geometry

Typically, the word geometry encompasses hole shape (cylindrical, laterally diffused, forward diffused, and laterally & forward diffused), hole arrangement (in-line, stagger, hole spacing, row spacing) and length to diameter ratio (l/d).

2.2.1 Single row geometry

Hole shape has always been a major focus of research for effectiveness

augmentation. Study on simple cylindrical holes and compound cylindrical holes are favored owing to their ease of manufacturing. Figure 3 highlights the two angles (α, β) that describe compound hole geometry.

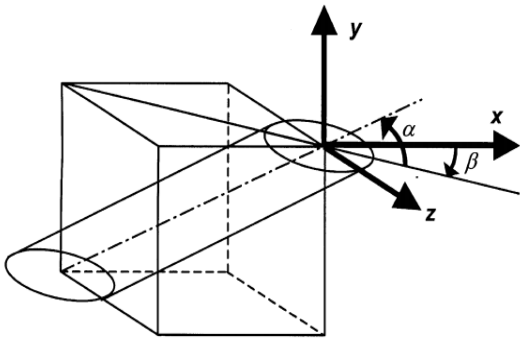

Figure 3: Compound angle hole configuration [10]

Goldstein [11] investigated a single row of simple cylindrical holes and compared with slot. It was observed that, at same blowing ratio, discrete holes provided lower effectiveness owing to jet penetration and lift off. However, the mechanical integrity of blade limits the use of slots. In another study, he compared single row of shaped holes (10^o lateral expansion) with simple cylindrical holes to further study the impact of shape and blowing ratio [12]. Shaped hole provided better lateral effectiveness and delayed lift off due to retarded momentum at the hole exit. Similar observations were made by Schmidt et. al [13], Sen et al. [14] and Taslim et. al [15] who compared compound holes and shaped holes with baseline case of simple cylindrical. All cases had similar effectiveness at lower blowing ratio; however for higher blowing ratio, compound shaped holes were generally found better than simple cylindrical. Between compound and shaped holes, due to expanded exit, latter demonstrated highest lateral distribution of jet with minimal lift off.

Baldauf et al. [16] adopted a more fundamental approach and investigated effect of stream angle, p/d, density ratio and blowing ratio for simple cylindrical holes. The author presented 0.8-1.0 as the optimum blowing ratio after which jet lift off was observed. A lower α resulted in better film coverage than higher α. Yuen et al. [17] also investigated effect of stream angle (α: 30º, 60º, 90º) for a simple cylindrical hole using Liquid Crystal Technique. A larger α assisted in coolant jet penetration into mainstream that resulted in jet lift off even for lower blowing ratios. Reducing the stream-wise angle gave better effectiveness and α: 30º was concluded as the most optimum of the three configurations. Also, for the same α, a higher blowing ratio gave a better effectiveness at larger x/d, owing to more coolant flow; however, increasing blowing ratio was generally observed to reduce the overall effectiveness for lower x/d.

Ekkad et al. [18] focused their study on the effect of compound angle (β = 0º, 45º and 90º) for cylindrical holes. Transient liquid crystal technique was employed with two density ratios. It was reported that compound angles provided a better effectiveness over simple cylindrical holes. Ligrani et al. [19] also used compound angle geometry (α: 24º, β: 50.5º). Higher effectiveness was explained by reduction in axial momentum and improvement in lateral momentum due to angle β which resulted in a better film coverage and delayed jet lift off. Comparable trends were reported by Nasir et al [20], for single row of compound holes (α: 55º, β: 0º, 65º).

To explain jet behavior, Vipluv et al. [21] used PIV to explain flow physics for compound angle holes (α: 30º) for two different β angles at different blowing ratio (1 and 2) and density ratio (1 and 1.5). Compound angles have vertical vorticity and lateral

vorticity. For lower β and higher M, the vertical component of vorticity is dominant which causes lift off. The converse is true for higher β angle. Larger, asymmetric vorticity allows for better lateral coverage, which is found aligned more towards the compound angle for higher M.

2.2.2 Multi-row geometry

Most of the studies discussed above used single row of cooling holes. In all cases, a sharp decay in effectiveness was observed downstream of injection hole due to film mixing in the mainstream flow. To sustain effective film coverage, multiple rows of holes need to be machined on the blade surface.

Ligrani et. al [22] recorded effectiveness for two row simple and compound angles. Effectiveness for two rows was reported to increase significantly for higher blowing ratios. Authors incorporated the effect of in-line / stagger arrangement of holes. Latter was found better than in line arrangement for all blowing ratios (0.2-0.6) while average effectiveness was observed to increase for increasing blowing ratio. Maiteh et al. [23] observed same trend for a combination of two row arrangements i.e. simple-simple, simple-compound and compound-compound holes. On similar lines, effect of having different hole geometry for row 1 and row 2 was investigated by Jubran et al. [24] by using simple cylindrical and shaped hole geometry with a density ratio of 1.7 using Infrared method. Effectiveness was found dominated by 2^{nd} row hole shape and average effectiveness was higher for two row case than one row. Additionally, it was

reported that hole spacing, arrangement and orientation significantly impacted the film distribution and resultant effectiveness.

Ahn et. al. [10] reported injection behavior from two row of compound angle holes with opposite orientation angles using Liquid Crystal Technique. Inline holes with (β: +45^o, -45^o) produced the highest effectiveness. Similarly, Kusterer et. al. [25] employed opposite orientation angles in two row arrangement to counter kidney vortex of coolant jet. The configuration (β: +45^o, -45^o) yielded highest effectiveness and lowest surface temperature. Other novel hole geometries incorporating anti-vortex holes branching out [26-28] are also available in open literature that are proven to increase cooling effectiveness by 30%-40% with half the original coolant consumption; however, manufacturing concerns limit their current use [29].

Very little literature has been found for three row case. Yang et al. [30] compared one row, two rows and three rows of cylindrical holes keeping coolant flow constant. Results showed maximum effectiveness with single row (d = 7 mm) followed by 3 row case (d: 3 mm). Effectiveness of all test pieces increased with increasing blowing ratio.

2.2.3 Hole spacing

Schmidt et al. [13] and Sen et al. [14] studied the effect of doubling hole pitch from 3D to 6D on overall effectiveness, which was observed to decrease by half for higher P/D ratio. For p/d of as low as 3, jet behaved independently and superposition principle could predict the effectiveness. Similar conclusion was presented by Baldauf et al. [31] for p/d of 2, 3 and 5. p/d 2 produced a uniform film more in line with slots, p/d 3

and 5 resulted independent jets. Han et al. [32] compared applicability of superposition principle on single row and two row case (α: 35°, β: 0°) for p/d 2.5. Lower blowing ratio (M 0.2) yielded comparable effectiveness values for two row design and one-row effectiveness based on superposition. For higher M, two row resulted in more than 60% increase in effectiveness explained by better cohesive coolant film less susceptible to be affected by mainstream.

Jubran et al. [33] investigated the effect of row (s/d: 4d, 10d) and hole spacing (p/d: 3d, 5.4d) on two row cylindrical hole (α: 30°, β: 90°) configuration. Effect of s/d was found more pronounced at low x/d while further downstream, the effectiveness was almost similar due to spreading of jet; flow regime is more 3-D near the injection hole becoming more 2-D with increasing x/d. Increasing p/d generally resulted in a decrease in effectiveness for all x/d at all blowing ratios. In another study, with α: 35°, β: 30° and 90°, Jubran et al. [34] varied p/d and s/d between 6-12 and 4-8 respectively to study the impact on overall effectiveness and presented film cooling correlations.

Mayle et al. [35] studied hole spacing (p/d) and blowing ratio effect for compound angle (α: 30°, β: +45, +45, +45) in staggered arrangement. Increasing p/d caused a reduction in effectiveness as amount of coolant available per unit area was decreased. However, the author argued that for high enough p/d, each jet behaves independently and principle of superposition may be employed to estimate average effect. For lower p/d, jet coalescence changes the behavior of film and how it interacts with mainstream, causing non-linear reduction in effectiveness due to variation in p/d.

2.2.4 Length to diameter ratio

L/D is either categorized as long (~ 6 and above), atypical to gas turbine blade or short (~1.5-4), representative of actual blade design. Both designs have different velocity profiles at hole exit. Burd et al. [36] explored the effect of turbulence and l/d ratio on jet behavior using a hot wire. For high turbulence, the effect of l/d is diminished. However, for lower free stream turbulence intensity, l/d effect is substantial as flow from smaller l/d injects farther in the span wise direction. In another study, Lutum & Johnson [37] reported negligible effect of l/d for l/d > 5 in case of cylindrical holes. Same result was reported by Gritsch et al. [38] for shaped holes.

2.3 Coolant / Mainstream Conditions

Coolant / Mainstream conditions refer to blowing ratio, density ratio and mainstream turbulence effects.

Owing to difference in mainstream and coolant air, the density ratio in actual gas turbines is typically 2.0. In general, increasing density ratio augments the film cooling effectiveness especially for high blowing ratios because it tends to stick to the surface of the test section [29]. This results in a delayed lift off at higher blowing ratio. Pederson et al. [39] studied density ratio effect from 0.75 – 4.17 for simple cylindrical holes (α: 30^o) and observed a substantial increase in effectiveness for higher density ratio at M =1.

To achieve different density ratios, researchers typically cool the coolant, heat the mainstream or use a foreign gas. Sinha et al. [40] used a chiller to achieve density ratio of 1.2, 1.6 and 2.0. The optimum blowing ratio was reported at 0.5-0.8. Ekkad et al.

[18] and Wright et. al [41] used foreign gas (CO_2) as coolant for density ratio of 1.5 to study compound angle effect on flat plate. Chen et al. [42] also employed CO_2 (DR 1.5) and mixture of SF_6 and Ar (DR 2.0) to investigate four different hole geometries.

For turbulence, enhanced turbulence encourages mixing of coolant jet into mainstream resulting in reduced effectiveness, especially at large x/d. However, closer to injection hole, in case of lift off condition, the turbulence helps bring the jet back to surface improving the film coverage [42].

3. RESEARCH OBJECTIVE

A wide array of parameters has been previously studied for single row and two row designs; however, information pertaining to three row is almost non-existent in open literature. Objective of the current study is to present complete information for a three row compound hole design including effect of orientation angle, inline – stagger arrangement, p/d ratio, blowing ratio and density ratio. Results will be presented in the form of effectiveness contours and graphs drawing comparisons and general trends for the studied parameters. This data may be used to compare new experimental results, build future numerical models or develop correlations. Design parameters may be optimized for application on turbine blades or even other gas turbine components like combustor liners, where multi row designs are more common.

4. EXPERIMENTAL SETUP

4.1 Instrumentation

Experiments were run on a suction type, low speed wind tunnel assembly. A schematic of the assembly is given in Figure 4 while Figure 5 and 6 are Solid Works models of the test section.

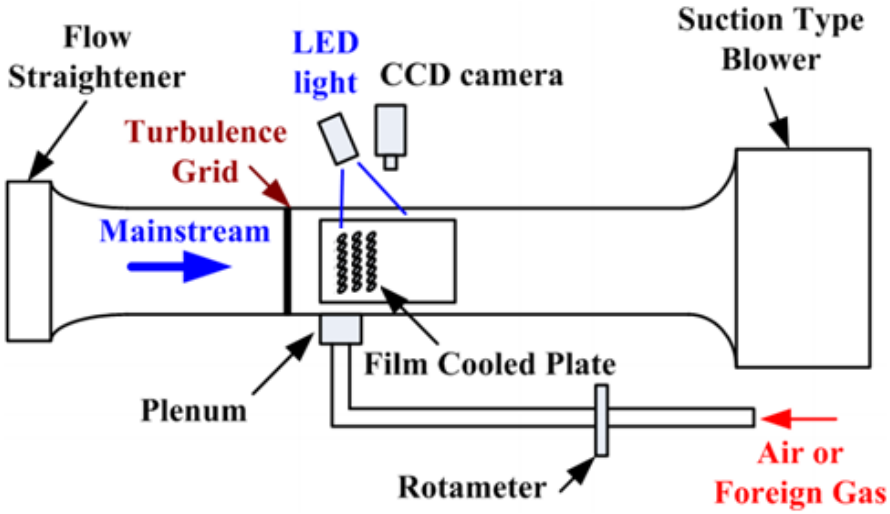

Figure 4: Schematic of wind tunnel apparatus [42]

4.2 Wind Tunnel

The wind tunnel entrance has a 4:1 contraction ratio with a 30.48 cm (12”) by 15.24 cm (6”) test channel. A 5.6 kW blower installed downstream of the test section maintains a constant mainstream flow. A turbulence grid installed at the entrance of test section provides a turbulence intensity of 6%. 0.635 cm (0.25”) diameter aluminum rods are arranged in a square mesh configuration with centerline spacing of 2.54 cm (1”); detailed design of turbulence grid is given in Young et al. [43]

A centerline mainstream velocity of 21.8 m/s was kept for all the test cases. Corresponding Reynolds number was 285,000 based on centerline velocity and hydraulic diameter of tunnel.

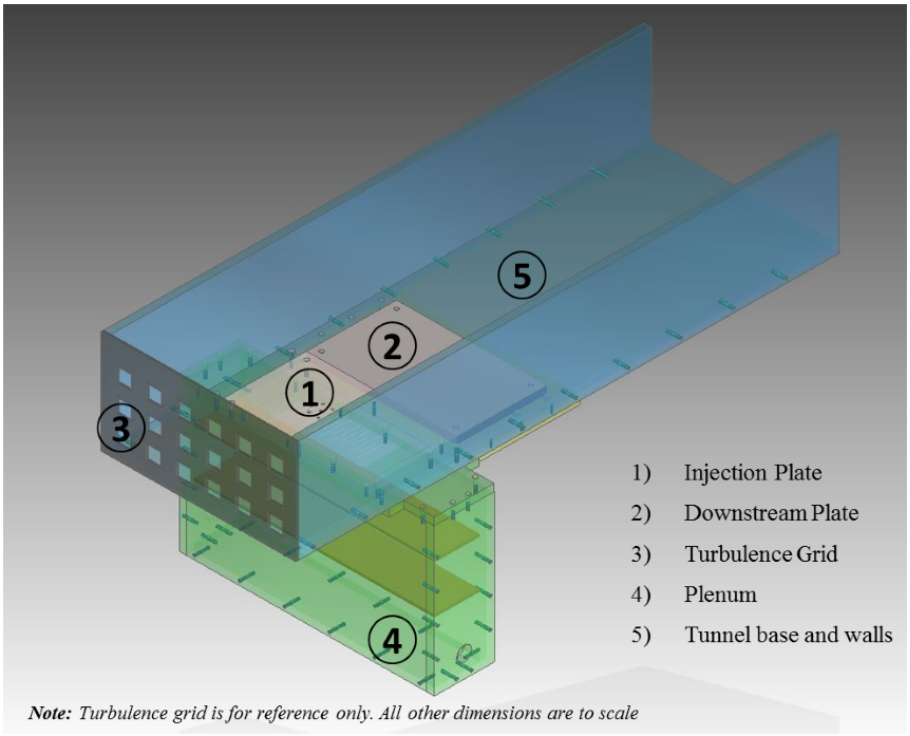

Figure 5: Isometric view of wind tunnel test section

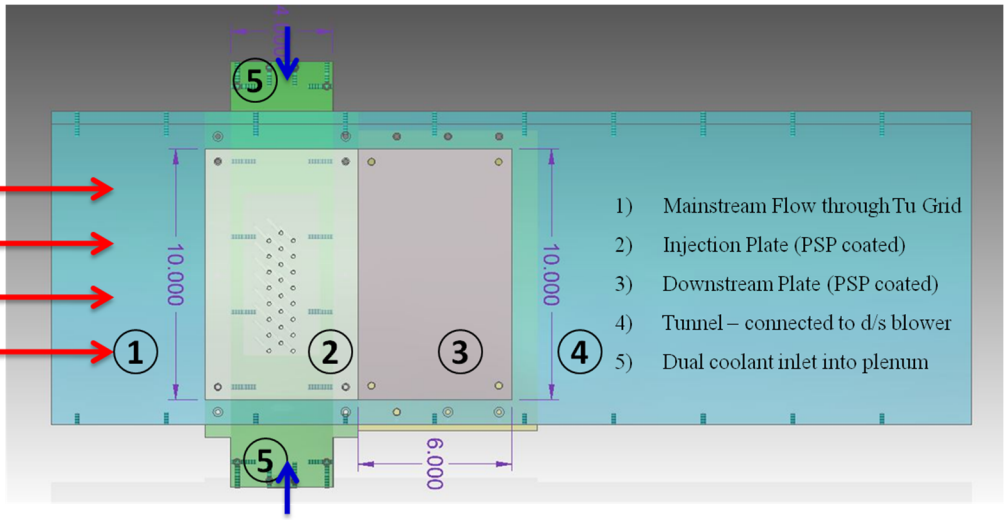

Figure 6: Top view of wind tunnel test section

4.3 Plenum

Plenum represents coolant passage that supplies coolant to the film cooling holes. It is fabricated of 1.27 cm (0.5”) thick Garolite G7 (green glass), 9.5” x 3” x 16” internally. Two 1” nps inlets are provided on either side of the plenum. Further, two wire meshes with 0.018” wire diameter and 0.045” open width (51% open area) are installed 1.5” and 3” above the inlets respectively. This is followed by 0.5” honeycomb to straighten the flow. Three 1/16” pressure taps are also given on each side of plenum to measure internal pressure and ensuring uniform internal flow. Injection plate is screwed directly on to the plenum surface. Internal details of the plenum are given in Figure 7.

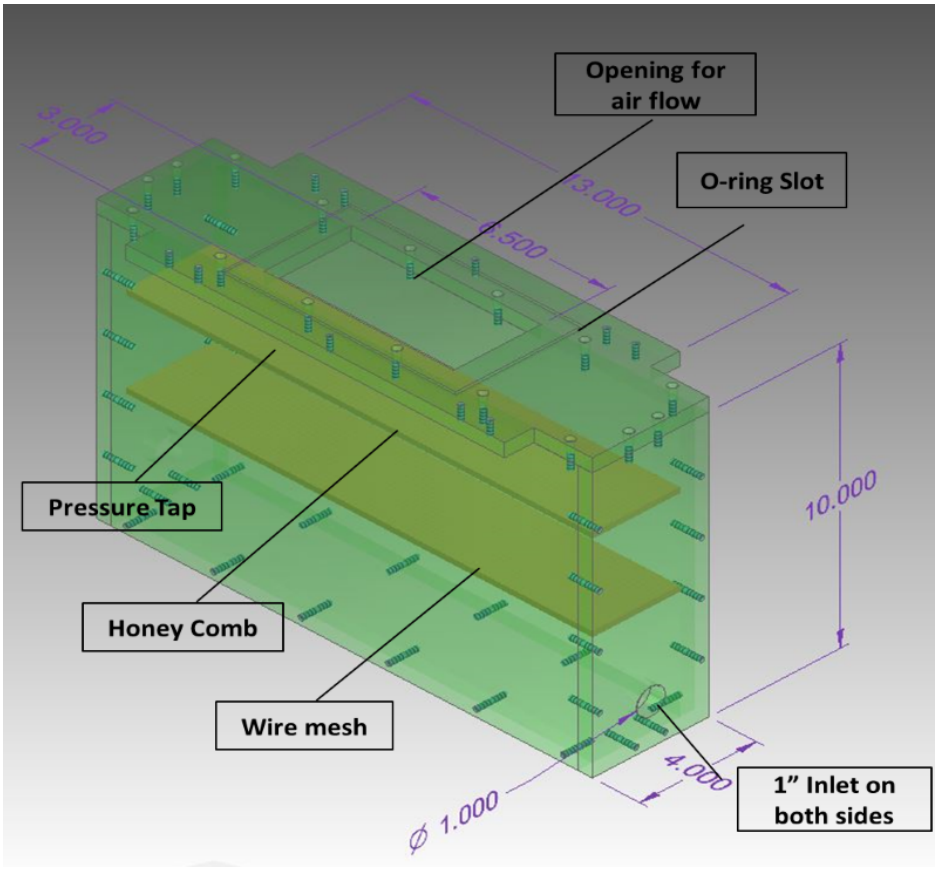

Figure 7: Isometric view of plenum and its internals

Coolant is supplied from compressor (air) or gas cylinders (N_2, CO_2, mixture of SF_6 & Ar). Coolant flow is regulated by Dwyer rotameters.

4.4 Injection Plate

The injection plate was screwed to the plenum top making it flush with the tunnel surface. An O-ring installed on the plenum ensured a perfect sealing. To confirm zero leakage, soap test was conducted after changing each injection plate. Test plate was sprayed with UniFib-750 procured from Innovative Scientific Solutions, Inc. ISSI Dayton, OH.

Even though there is no specific restriction on base material usage for PSP as long as calibration is being done, Polyurethane Last A Foam Series by General Plastics was chosen due to its low conductivity and potential future studies on the same plates using other heat transfer methods (IR, Liquid Crystal, TSP etc.)

4.5 Test Matrix

Eight plates were machined, four each of p/d 4 and 6 while p/d 8 was obtained by blocking alternate holes on plate with p/d of 4. A total of 180 cases were run as shown in Table 1. Figure 8 is a schematic of hole geometry for p/d 4 (only four of six holes per row are shown). Mainstream flow parameters are summarized in Table 2.

Table 1: Test matrix for 180 cases

Case	Geometry (hole diameter: 4 mm)								Coolant Flow Parameters	
	α	Row 1 β	Row 2 β	Row 3 β	Arrangement	p/d	s/d	l/d	M	DR
A	30º	45 º	45 º	45 º	In line	4 , 6, 8	3	6.3	0.5, 0.75, 1.0, 1.25, 1.5	1, 1.5, 2.0
B	30 º	45 º	45 º	45 º	Row 2 & 3 staggered					
C	30 º	45 º	-45 º	-45 º	In line					
D	30 º	45 º	-45 º	-45 º	Row 2 & 3 staggered					

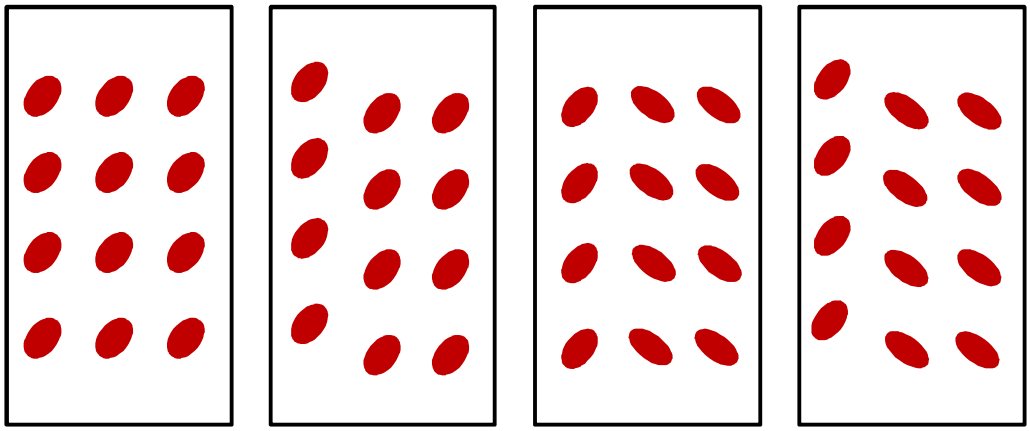

β = +45, +45, +45 **A (**in line) | β = +45, +45, +45 **B** (stagger) | β = +45, - 45, - 45 **C** (in line) | β = +45, - 45, - 45 **D** (stagger)

Figure 8: Hole arrangement for p/d: 4

Table 2: Mainstream flow parameters

Mainstream Flow Parameters	
Density	1.142 kg/m^3
Temperature	298 K
Velocity	21.8 m/s
Reynolds Number	285,000
Turbulence	6 %

5. EXPERIMENTAL METHOD

Pressure Sensitive Paint was used to record film effectiveness data. It is a mass-transfer technique, developed by Zhang and Jaiswal and Zhang and Moon [44]. Since then, it has been widely accepted as a viable experimental method to measure adiabatic film effectiveness over flat plate, cylinders, leading edge etc. [11, 42, 44].

5.1 Principle

PSP is a photo luminescent material that emits light with intensity proportional to surrounding partial pressure of oxygen via a process called oxygen quenching. Under the light source, the photo luminescent particles get excited and emit photons of longer wavelength when returning to original state. The emitted light is inversely proportional to the concentration of oxygen absorbed into the PSP binder. A calibration for intensity versus partial pressure gives the pressure information which can be used to find overall effectiveness.

Typically, the test piece is first painted black followed by 6-9 coats of PSP in cross pattern using air brush and nitrogen media to attain a uniform finish. In current set up, PSP was excited using 400 nm LED light source and images captured from a Sensi Cam CCD camera with a 600 nm long pass filter. Figure 9 shows a schematic of PSP principle.

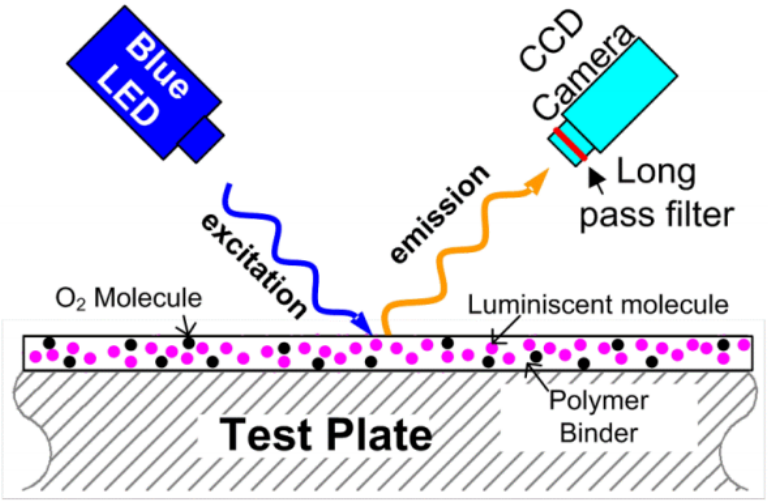

Figure 9: Schematic of PSP paint principle [42]

5.2 Calibration

PSP calibration was carried out by painting a small test piece and placing it inside a vacuum chamber. Figure 10 shows calibration set up for the experiment. 29 in of Hg (corresponding to ~ 0.031 atm) was achieved using vacuum pump and 200 images recorded by CCD camera. These images were averaged to cancel camera noise. The step was repeated for a range of vacuum pressures (at increments of 2 inches of Hg) and corresponding intensity images saved including reference image at ambient pressure. The intensity at each pressure was normalized by reference intensity to eliminate any effect of paint non-uniformity.

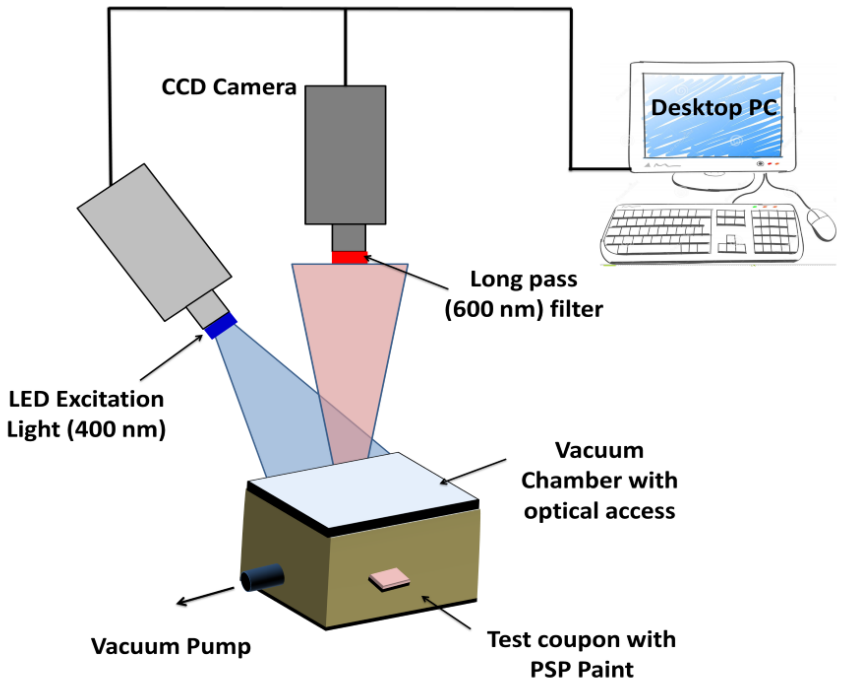

Figure 10: PSP paint calibration set-up

Three different paint bottles for PSP paint (UniFib 750) were available in Turbine Heat Transfer Lab's inventory. Calibration was carried out for each before proceeding with data acquisition and reduction. The curves are plotted in Figure 11.

5.3 Data Acquisition

A typical run on PSP comprises of four image sets: air image (oxygen rich environment, light on, mainstream flow on), coolant image i.e. N_2, CO_2, mixture of SF_6 & Ar (oxygen quenched environment, light on, mainstream flow on), reference image (no coolant flow, light on, mainstream flow off) and black image (no coolant flow, light

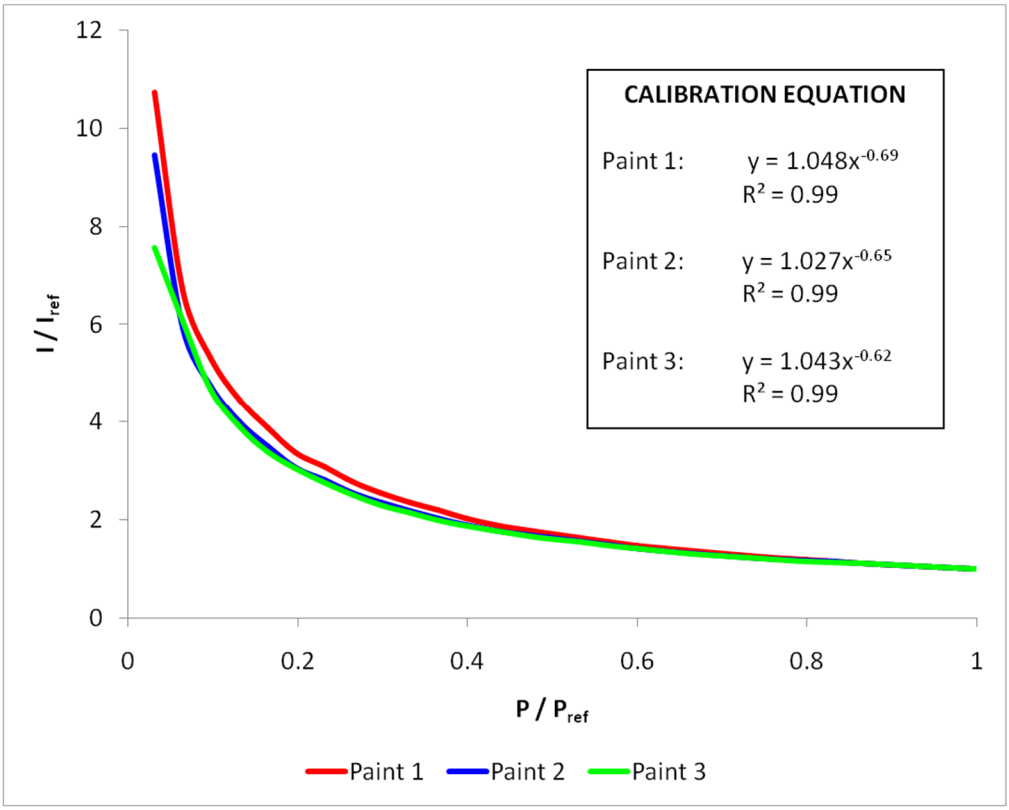

Figure 11: PSP paint calibration curves

off, mainstream flow off). The reference image is required to normalize the intensity image while black image cancels background noise.

Since PSP is a mass transfer technique, effectiveness is given by:

$$\eta = \frac{T_{aw} - T_m}{T_c - T_m} = \frac{C_w - C_m}{C_c - C_m} = \frac{P_{O_2}\ air - P_{O_2}\ fg}{P_{O_2}\ air}$$

where c, m and w are oxygen mass fraction in coolant, mainstream flow and plate wall.

When density ratio is other than 1, following formula needs to be used:

$$\eta = 1 - \frac{1}{\left(\frac{P_{O_2 air}}{P_{O_2 fg}} - 1\right) * W_{fg}/W_{air} + 1}$$

6. RESULTS

Effectiveness contours and span-wise average data plots for important cases are discussed here. Contours are presented for middle three holes only while effectiveness average is taken for middle two holes as shown in Figure 12. Care was taken to avoid the edge effect.

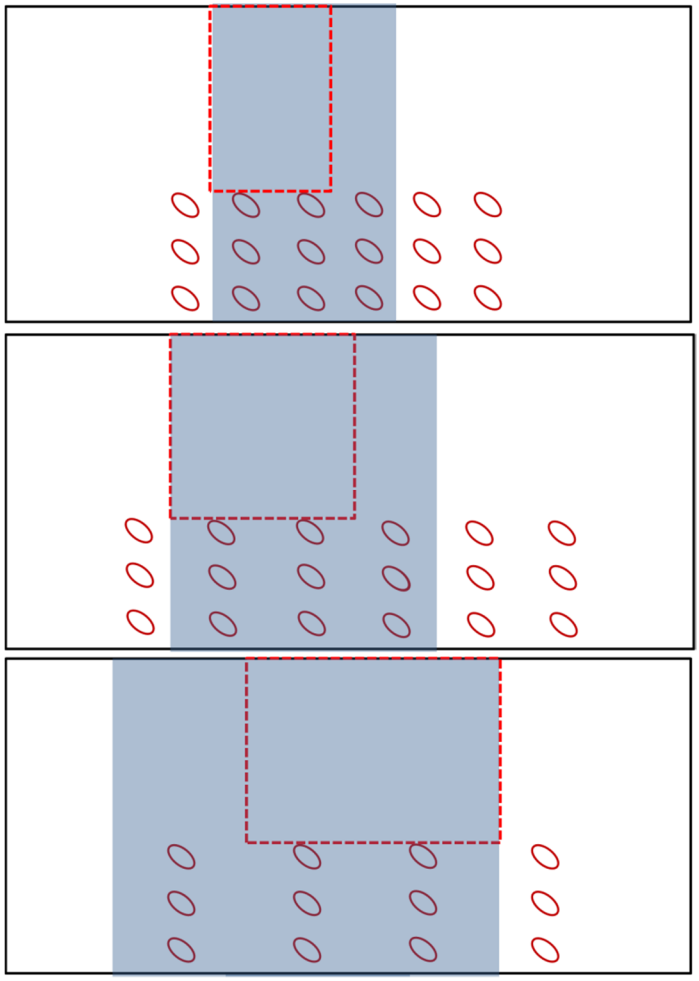

Figure 12: Sketch showing contour region (greyed), average effectiveness region (dotted) for p/d: 4, 6 and 8 (top to bottom)

As discussed previously, p/d 8 was obtained by blocking alternate holes on plate with p/d 4. These covered holes appear as uniformly colored (blue / green) regions in the contours owing to presence of fluorescence in the clay dye which gets excited under LED light. It is noteworthy that these regions do not represent any data. Moreover, being flush with plate surface, contours illustrate that these blocked holes provide no interference to coolant jet or mainstream flow.

The data taking region was fabricated in two separate parts: the injection plate and downstream plate. This allows replacement of only the injection plate (x/d 10) while keeping downstream plate (x/d ~35) in place. It helps optimize the assembly time as well as PSP paint usage. The small gap between both is covered by 3-4 mm of commercially available scotch tape. This region appears as clear blue line in the contours representing "no data". Even though the effectiveness contours present uniform flow over this region, it is believed the coolant flow may still have been impacted due to tape step; it was decided not to report data for x/d 1 upstream and downstream of the tape together with the tape region itself. This appears as a discontinuity in effectiveness plots.

6.1 Comparison with Open Literature

Little data is available for three row flat plate film cooling in open literature. The two papers encountered [35, 36] were found to have different geometrical and flow parameters hence a comparison is not justified. However, to ascertain accuracy of data, all runs were repeated several times on same day as well as different dates and found to be repeatable.

6.2 Effect of Geometry (orientation angle / inline – stagger)

Keeping p/d constant at 4 and DR at 1, Figure 13 shows the effect of orientation angle and hole arrangement (inline – stagger) with increasing blowing ratio.

For x/d <3, plate (a) shows a decrease in average effectiveness with increasing M. This is due to lift off effect which is initiated at M: 0.75; higher momentum of jet allows it to penetrate more into the mainstream flow causing separation. Re-attachment is observed at x/d: 3-5 (greater re-attachment length at higher M), resulting in an elevated effectiveness at this location. M 1.5 results in a consistently better film coverage at x/d >10 attributed to higher coolant flow per unit area. However, moving downstream, overall effectiveness undergoes a sharp decay until all blowing ratios converge to a point as jet spreads and mixes into mainstream flow.

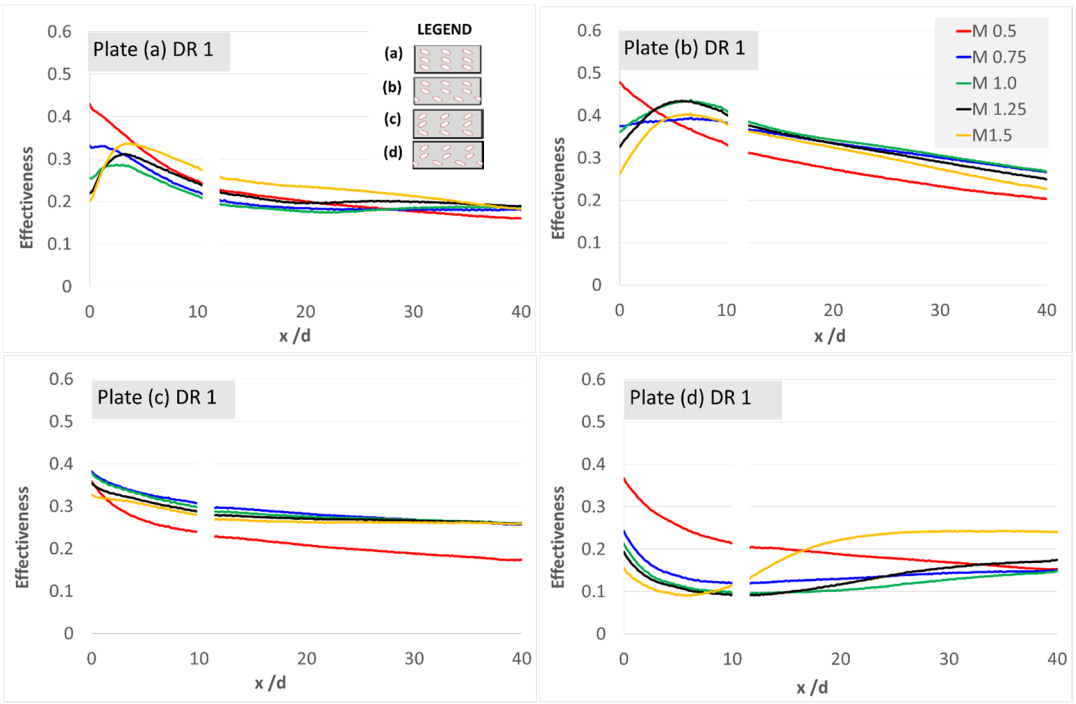

Figure 13: Effect of hole orientation/angle on average effectiveness with increasing blowing ratio for p/d 4

Similar trends are observed for Plate (b), which has same orientation angles as plate (a) except row 2 and 3 are staggered. For lower x/d, highest effectiveness is observed at M: 0.5 decreasing substantially with increasing blowing ratio due to lift. Re-attachment occurs at x/d: 8-10, farther down than plate (a) probably due to compound effect of stagger arrangement that imparts greater stream-wise momentum to jet. Unlike plate (a), effectiveness of M 0.5 is significantly lower for large x/d than for other blowing ratios. Comparing both, plate (a) and (b), stagger arrangement results in an increased overall effectiveness due to better distribution of jet on flat plate surface.

Plate (c) has an inline design with opposing orientation angle for row 1 and row 2/3. This is the only three row design studied that conforms to effectiveness versus blowing ratio trend for single row design found in literature. With increasing blowing ratio, larger amount of coolant is available; the average effectiveness is found to increase until M 1.0 thereafter it decreases due to lift off. The effectiveness values merge at x/d 30.

Results for plate (d) are found significantly lower than plate (c) for all blowing ratios except M 0.5. This is contrary to the general trend that stagger arrangement yields better coverage. In fact, this proves the strong correlation between hole arrangement (stagger-in line) and orientation angle. Compound effect of opposing jets increases vertical and stream-wise momentum resulting in early – longer – lift off even at lower blowing ratios. This behavior of orientation angle agrees with findings of Ahn et al. [27] who explained it in terms of downwash and up wash flow effect on lift off for two row design. Re-attachment occurs at very large x/d ~20, post which point, M1.5 gives highest

effectiveness value. Comparing the four designs, (b) gives the highest average effectiveness followed by (c) for all blowing ratios.

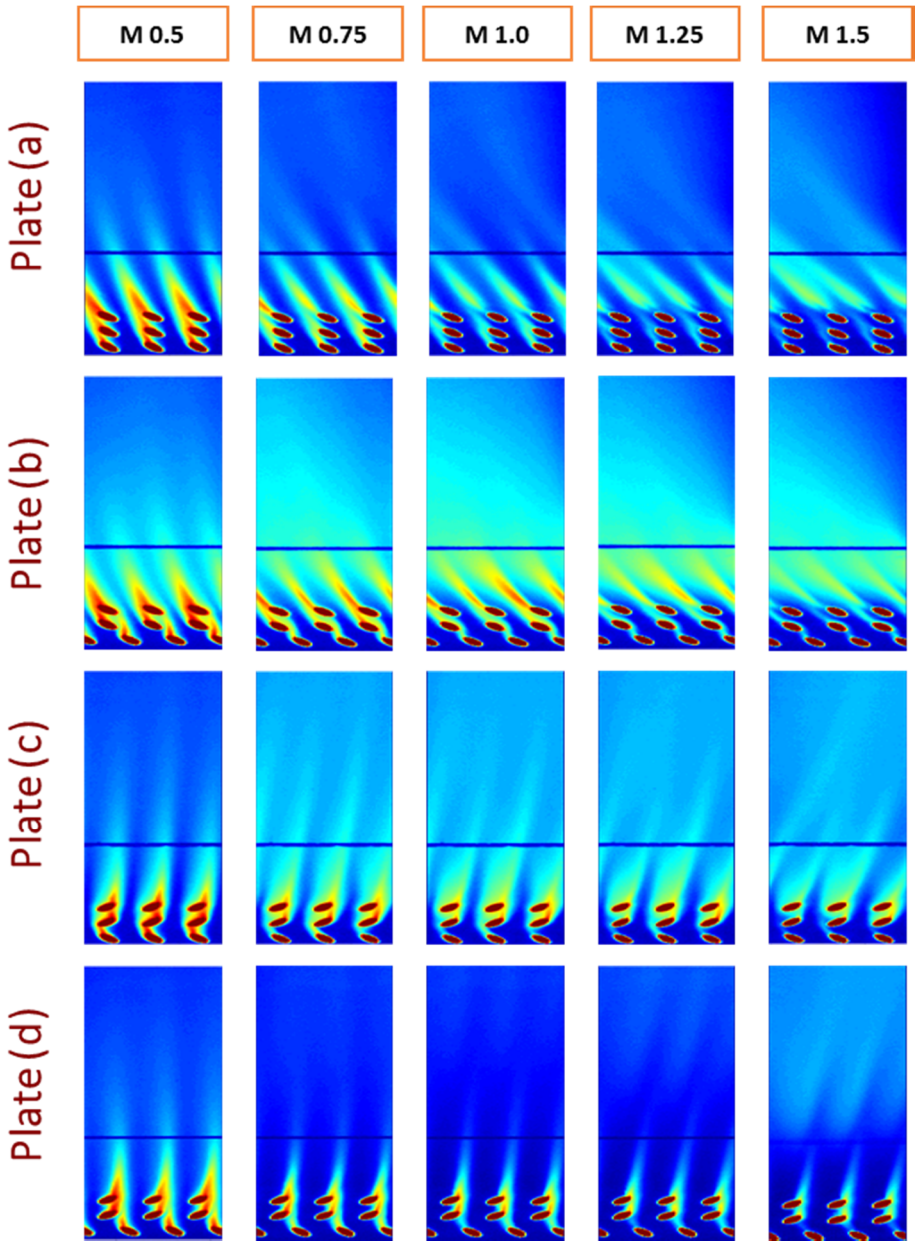

Figure 14: Effectiveness contour for hole orientation / arrangement (p/d 4, M: 0.5-1.5)

6.3 Effect of Density Ratio

Detailed film cooling effectiveness for DR 1, 1.5 and 2.0, cases A-D for p/d 4 are given in Figures 15-18.

Generally, increasing DR is observed to increase the average effectiveness. This increment is larger for DR 1 to 1.5 than 1.5 to 2.0. In fact, for DR 2, there are cases where, for low blowing ratio, the effectiveness has decreased below that of DR 1.5. This is explained by the reduction in coolant momentum / flow rate out of the injection holes. However, for higher blowing ratio, significant increase is reported. In addition to more coolant being available per unit area, heavier coolant tends to stick closer to flat plate surface because of reduced momentum delaying lift off. Consequently, optimum blowing ratio is increased too. This difference is more evident for plate (a) and (d) which

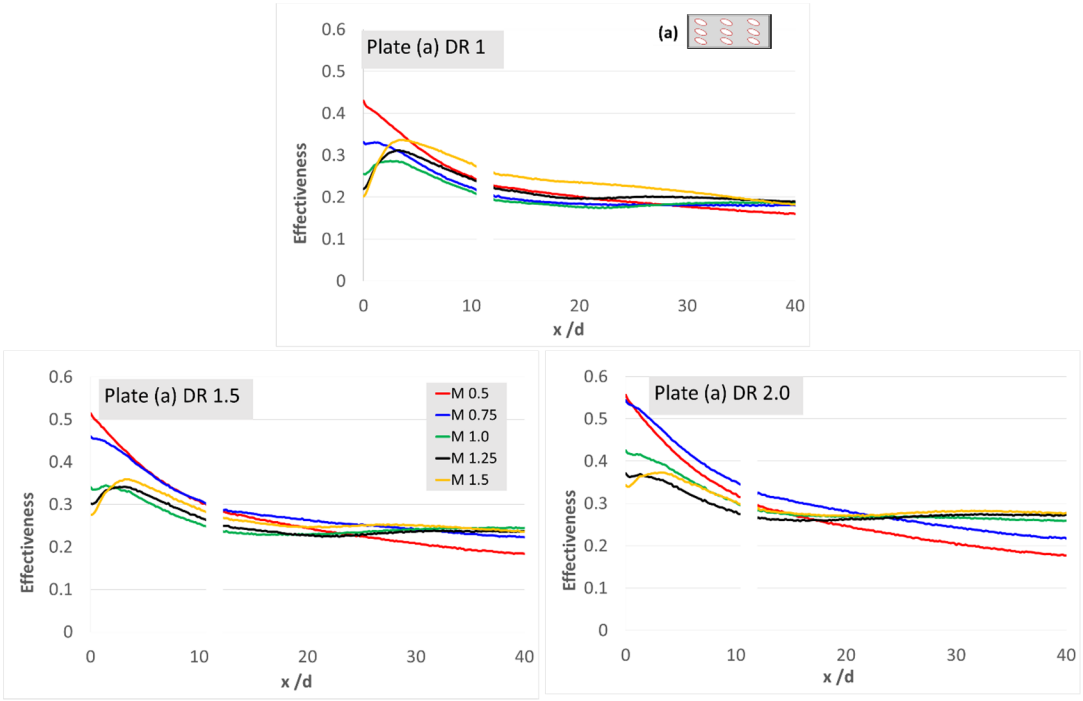

Figure 15: Effect of DR (1.0, 1.5, 2.0) on average effectiveness (Plate A) – p/d 4, with M (0.5 - 1.5)

experience more jet lift off than other designs. For same reason, DR effect is observed to have a larger influence at smaller x/d.

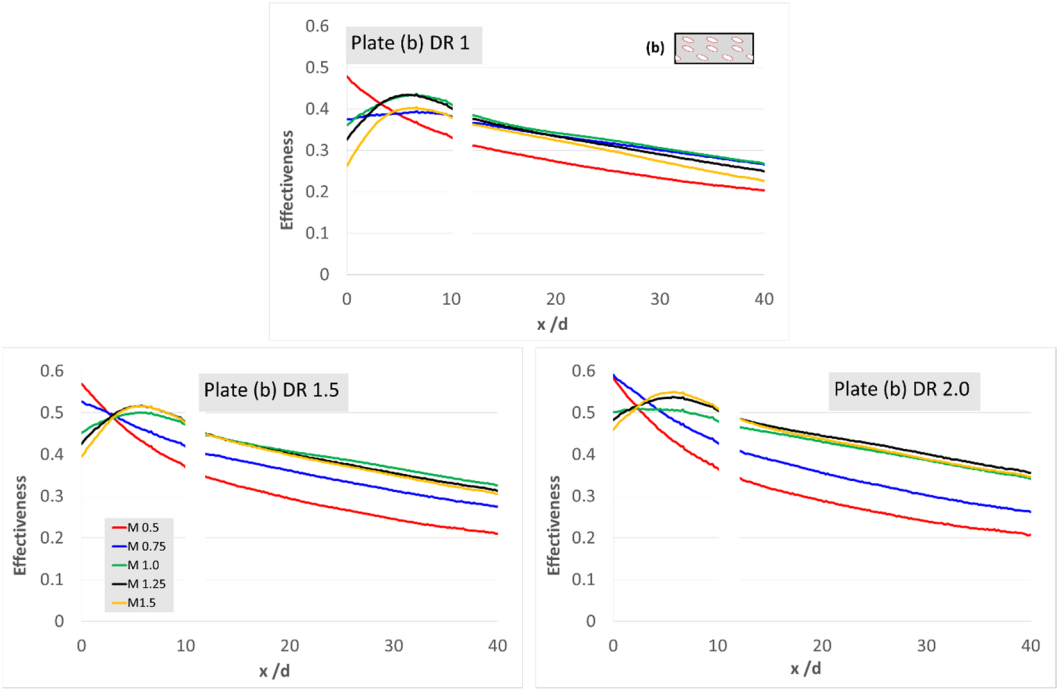

Figure 16: Effect of DR (1.0, 1.5, 2.0) on average effectiveness (Plate B) – p/d 4, with M (0.5-1.5)

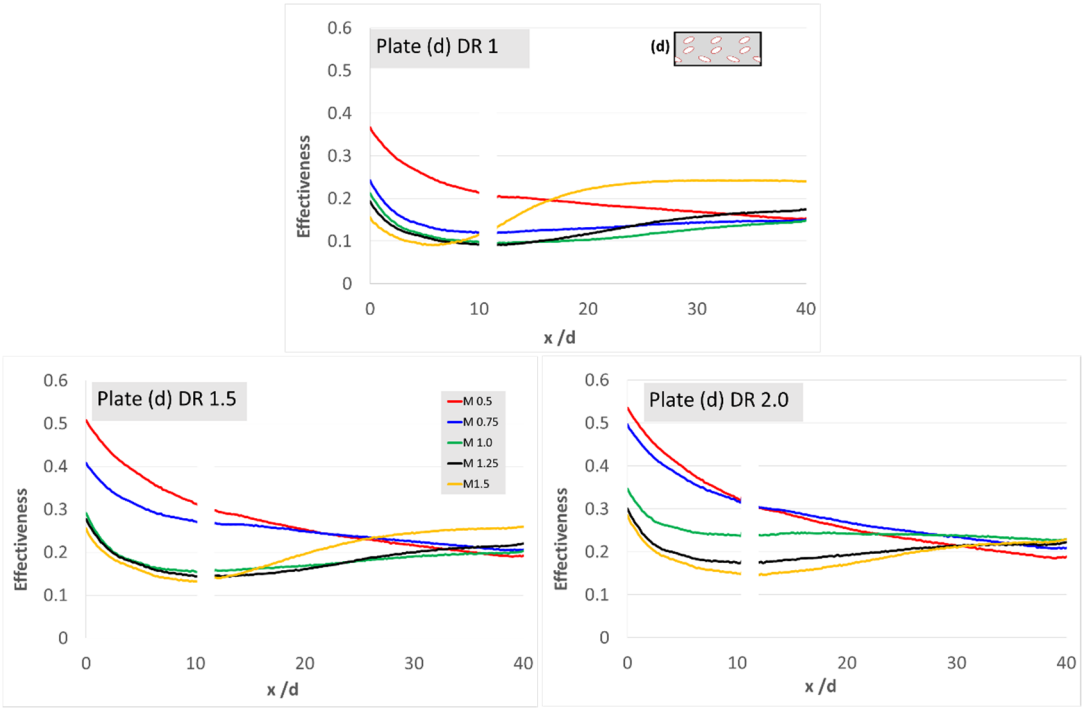

Figure 17: Effect of DR (1.0, 1.5, 2.0) on average effectiveness (Plate D) – p/d 4, with M (0.5-1.5)

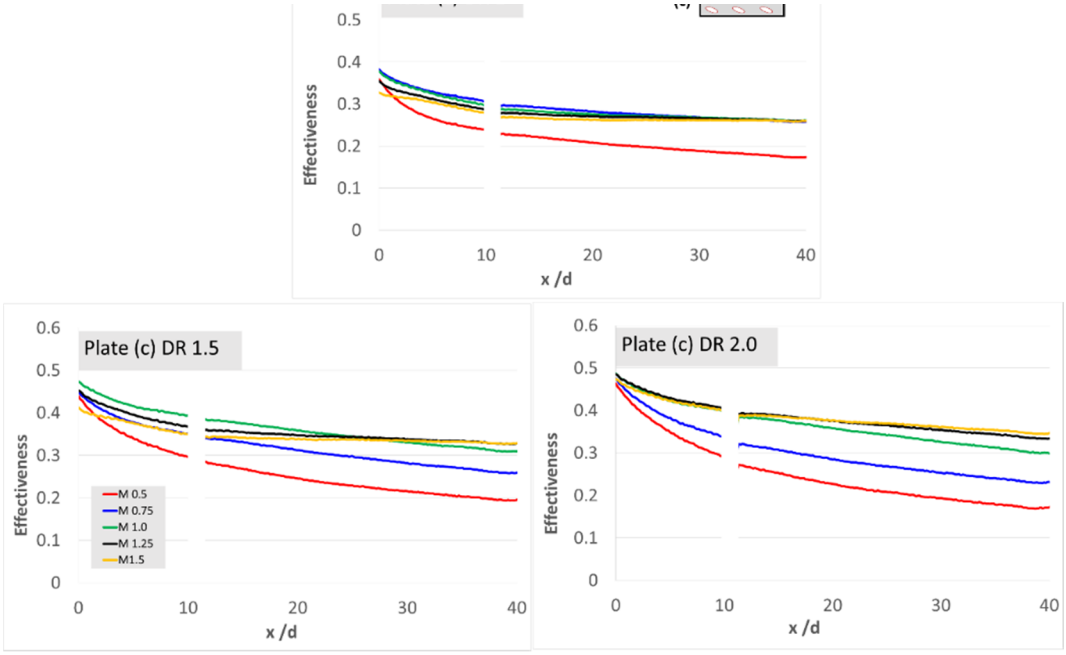

Figure 18: Effect of DR (1.0, 1.5, 2.0) on average effectiveness (Plate C) – p/d 4, with M (0.5-1.5)

6.4 Effect of p/d

Increasing p/d reduces overall effectiveness for all blowing ratios and density ratios. This can be explained by limited availability of coolant per unit surface area resulting in loss of film cooling particularly in regions between the holes. However, the reduction is not always linear i.e. doubling p/d does not necessarily half the effectiveness, which concludes that factors like jet coalescence and interaction play an integral role in film effectiveness.

Average effectiveness plots and contours for two representative cases (plate B and C) are given in Figures 19 to 22. Even though orientation angles / row arrangement are different, intent is to demonstrate how jet development impacts effectiveness with change in hole spacing.

Plate B contours show independent jets for low blowing ratio and smaller hole spacing; hence, increasing hole spacing results in relatively uniform reduction. This reverses as blowing ratio increase. For higher momentum flux, greater jet bending in direction of compound angle and general higher availability of coolant causes neighboring jets to mix. A distributed film is developed over the surface. Increasing hole spacing compromises this coalescence and reduces effectiveness substantially for hole spacing increase from 4 to 6. The effect is more evident for low $x/d < 15$. On the contrary, Plate C, which is an inline design, produces relatively independent coolant jets even for lower hole spacing, higher M. Therefore, variation in effectiveness with increasing p/d is somewhat uniform. Similar trends are observed for Plate A & D, comparison plots for which can be referred to in the Appendix.

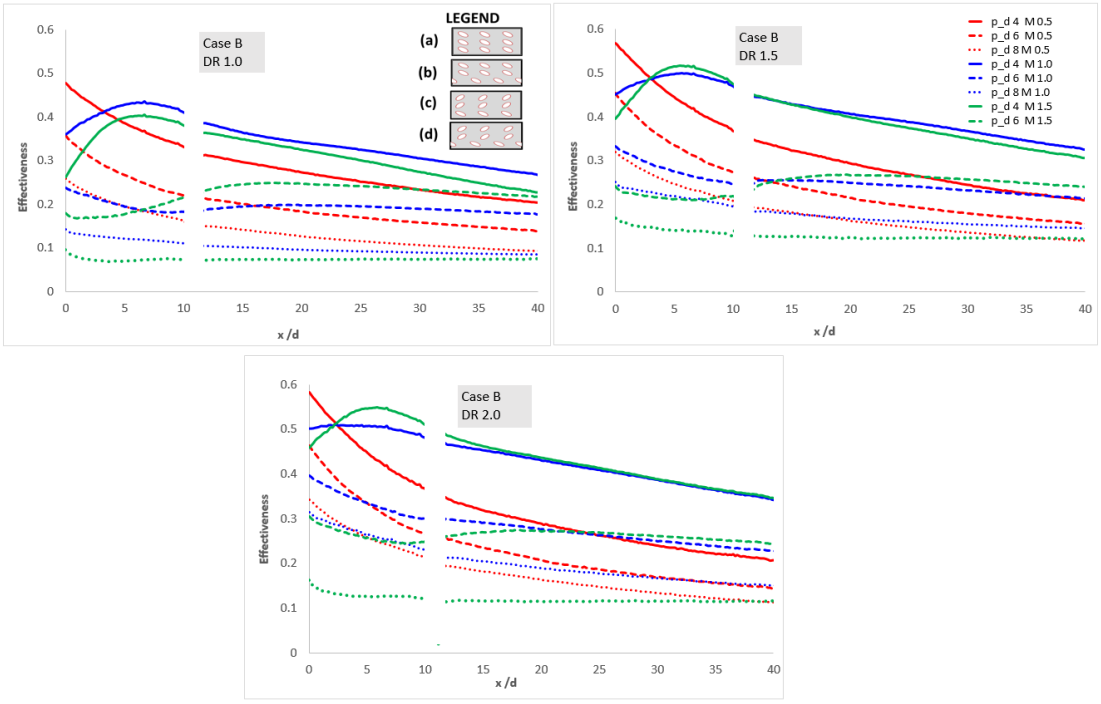

Figure 19: Effect of p/d on average effectiveness (Plate B) for different M and DR

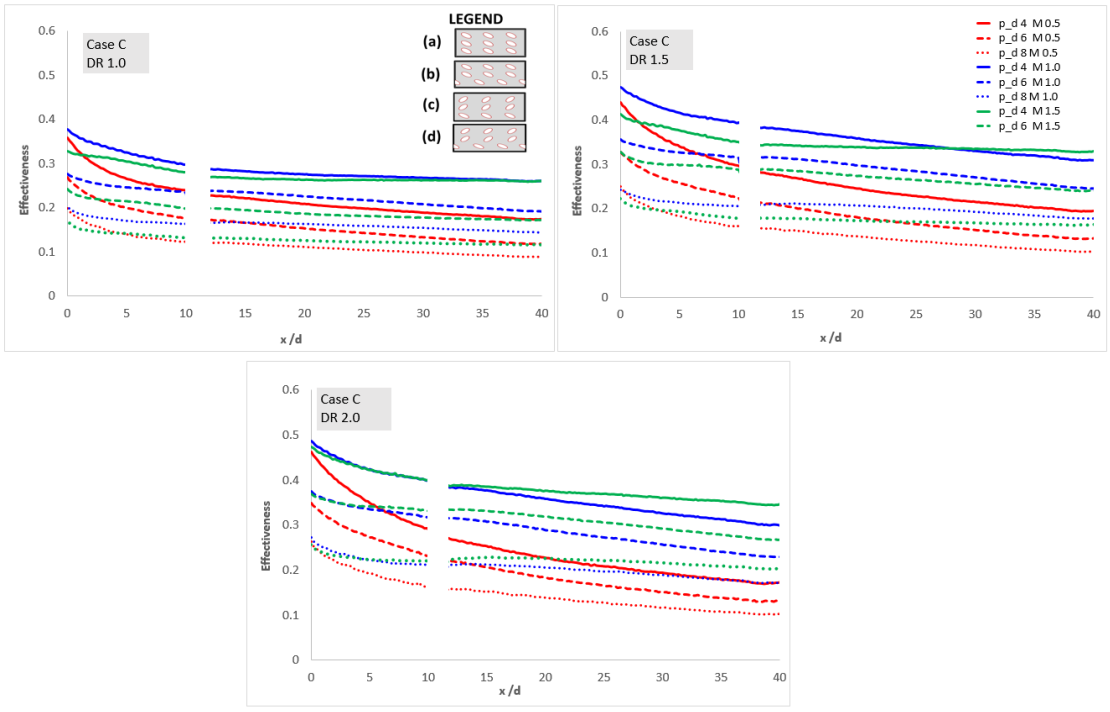

Figure 20: Effect of p/d on average effectiveness (Plate C) for different M and DR

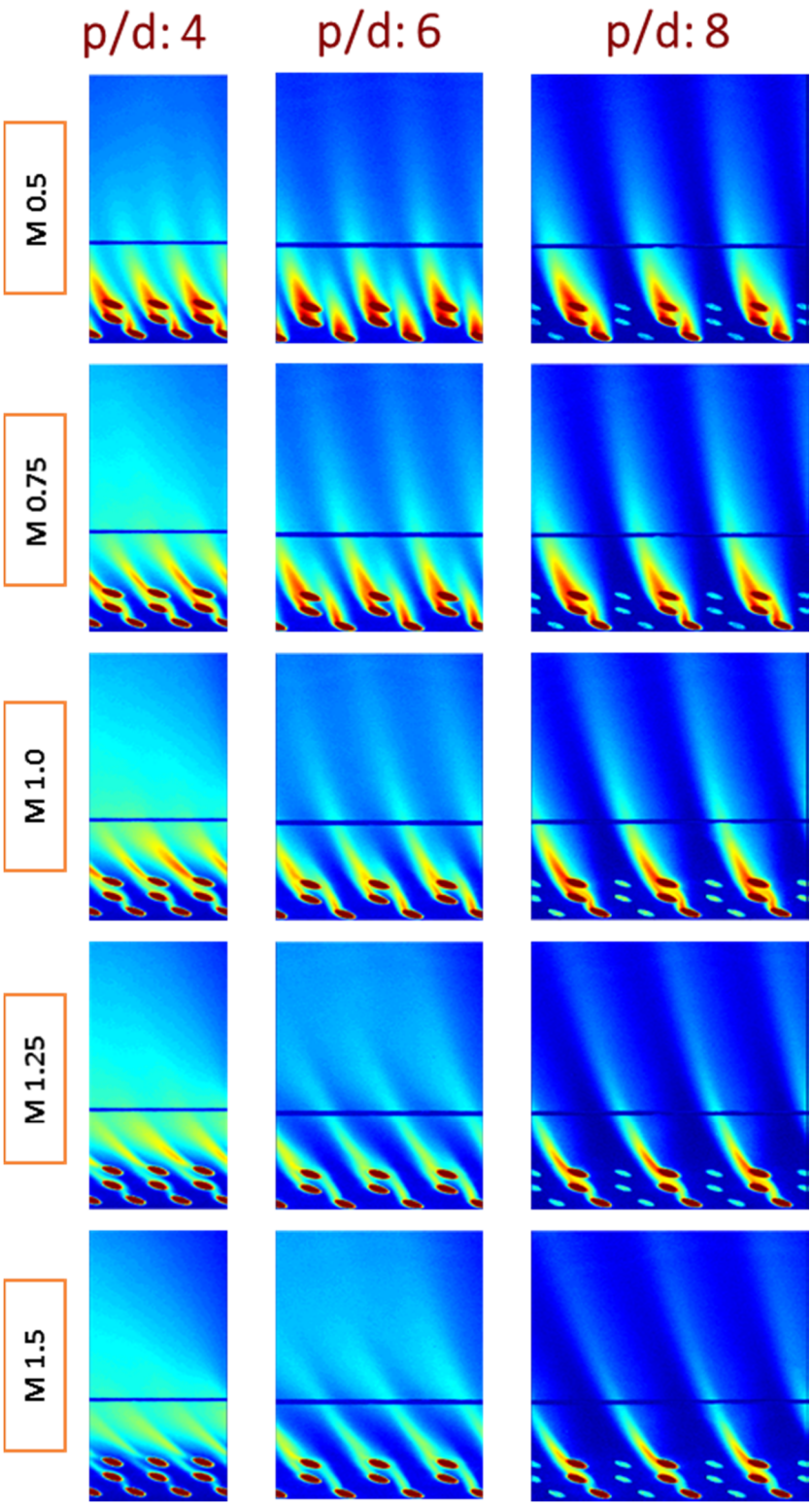

Figure 21: Effectiveness contour (Plate B) - DR 1.5 for increasing p/d & M

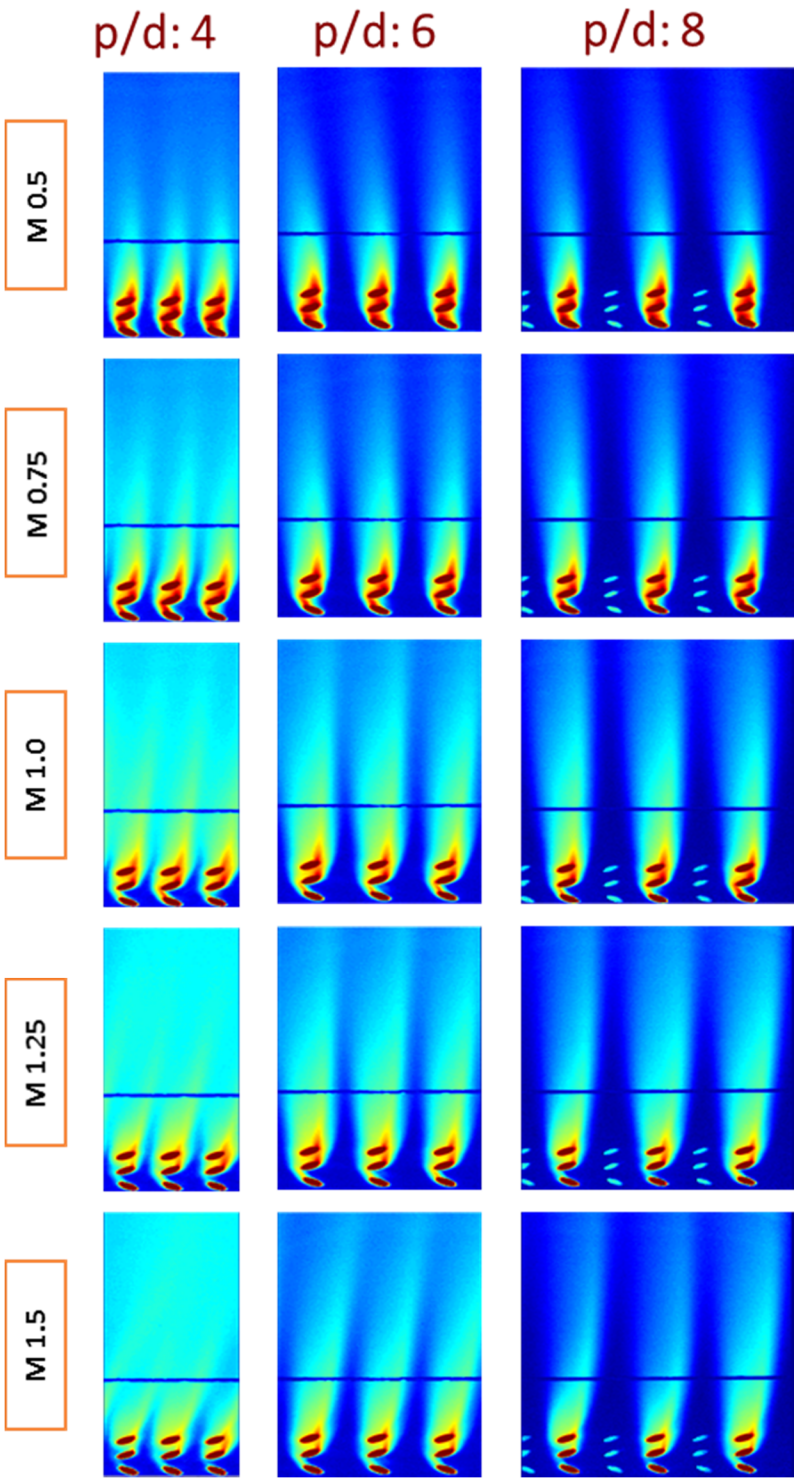

Figure 22: Effectiveness contour (Plate C) - DR 1.5 for increasing p/d & M

6.5 Uncertainty Analysis

Kline and McClinktock [45] approach is used to calculate uncertainty. From previous discussion, film effectiveness is primarily dependent on $PO_{2,fg}/PO_{2,ref}$ and $PO_{2,air}/PO_{2,ref}$, which is derived from the calibration curve; any uncertainty in calibration will contribute to the final result. Factors contributing to error include pressure measurement (0.1 in Hg) and bias error in pressure transducer (0.1 in Hg). While lighting condition was kept constant through the duration of calibration, any minor changes in temperature, ideally kept constant through buildings HVAC system are neglected.

During experimentation, error in velocity (2%) as well as managing coolant flowrate (±1 SCFH) also adds to the overall error. Any error in CCD camera (background noise) is reduced by averaging multiple images; it is noteworthy that camera error will be lower at higher intensity (corresponding to higher effectiveness) than at lower intensity. Moreover, issues in paint quality (non-uniformity, degradation over time etc.) are eliminated by normalizing intensity.

Based on previous studies carried on the same equipment by [42, 43], for η 0.3, the approximate uncertainty in pressure measurement is 1% and intensity ratio is 1% (estimated from multiple cases). Resultantly, PO_2/PO_{2ref} has an uncertainty of 3.3 % while overall effectiveness uncertainty is ~ 8%.

7. CONCLUSION

An experimental investigation on effect of different parameters on film cooling effectiveness was carried out for three rows of compound holes over a flat plate. Eight test sections were machined to run 180 cases using PSP technique. Results were generally found to be in good agreement with trends available in open literature. Following summarizes major conclusions:

7.1 Effect of Hole Orientation Angle / Arrangement

- Same orientation angle, stagger arrangement (Plate B) presents most optimum design followed by opposite orientation, in line design (Plate C). In both cases, the cascading jets complement each other for better coverage
- Opposing angles, staggered arrangement causes jet interference resulting in jet lift off / mixing into mainstream
- Hole orientation angle and arrangement have a combined effect on jet behavior; hence both need to be accounted for in multi-row design

7.2 Effect of Blowing Ratio

- No direct correlation found between blowing ratio and effectiveness
- Each design observed to be case specific as effect of increasing blowing ratio is found to be strongly dependent on the geometry.

7.3 Effect of Density Ratio

- Increasing DR improves η as heavier gas tends to stick to surface and delay lift off
- DR effect is more prominent at low x/d for same M. This difference is more evident for plate (a) and (d) which experience more jet lift off than other designs
- Effect of DR is more significant at higher M as more coolant flow imparts greater lateral momentum. At low M, flow rate is too small to produce substantial improvement

7.4 Effect of Hole Spacing (p/d)

- Increasing p/d decreases effectiveness for all blowing ratios; however, the decrement is not linear to p/d change
- Hole spacing effect is more substantial for low x/d and higher blowing ratios. Generally, at higher blowing ratios, in addition to hole spacing, effectiveness is dominantly affected by neighboring jet interaction

Even though three row design generally yields higher effectiveness than single or double row designs especially at larger x/d, it is pertinent to understand that design objective in practical application is to minimize coolant usage for the same or higher effectiveness. Future study for this experiment may focus on using similar geometrical parameters for one-row and two rows respectively for a comprehensive comparison.

Moreover, utilization of PIV or other flow measurement techniques can help explain the flow regime and consequently identify reasons for such sharp differences in effectiveness for different plate designs.

REFERENCES

[1] Han, J. C., 2013, “Fundamental Gas Turbine Heat Transfer” Journal of Thermal Science and Engineering Applications, 5(2)

[2] Han, J., Datta, S., and Ekkad, S., 2013, “Gas Turbine Heat Transfer and Cooling Technology”. 2nd ed. CRC Press/Taylor & Francis

[3] Gao, Z., 2007, “Experimental Investigation of Film Cooling Effectiveness on Gas Turbine Blades,” PhD Thesis, Texas A&M University, URL: http://oaktrust.library.tamu.edu/bitstream/handle/1969.1/ETD-TAMU-1557/GAO-DISSERTATION.pdf?sequence=1&isAllowed=y

[4] Goldstein, R. J, 1971, “Film Cooling,” Advances in Heat Transfer, 7

[5] Han, J. C., and Ekkad, S., 2001, “Recent Development in Turbine Blade Film Cooling,” International Journal of Rotating Machinery, 7(1), pp 21-40

[6] Bunker, R. S., 2005, “A Review of Shaped Hole Turbine Film-Cooling Technology,” Journal of Heat Transfer-Transactions of the ASME, 127(4), pp 441-453

[7] Bogard, D. G., and Thole, K. A., 2006, “Gas Turbine Film Cooling,” Journal of Propulsion and Power, 22(2), pp 249-270

[8] Han, J. C. and Rallabandi, A. P., 2010, “Turbine Blade Film Cooling using PSP Technique,” Frontiers in Heat and Mass Transfer, 1(1)

[9] Kianpour, E., Sidik, N. A. C., and Golshokouh, I., 2014, “Film Cooling Effectiveness in a Gas Turbine Engine: A Review,” Jurnal Teknologi, 71(2), pp 25-35

[10] Ahn, J., Sung Jung, I., and Lee, J. S., 2003, “Film Cooling from Two rows of Holes with Opposite Orientation Angles: Injectant Behavior and Adiabatic Film Cooling Effectiveness,” International Journal of Heat and Fluid Flow, 24, pp 91-99

[11] Goldstein, R. J., Eckert, E. R. G., Erikson, V. L., and Ramsey, 1970, “Film Cooling Following Injection through Inclined Circular Tubes,” Israel Journal of Technology, 8, 135.

[12] Goldstein, R. J., Eckert, E. R. G. and Burggraf, F., 1974, “Effects of Hole Geometry and Density on Three-Dimensional Film Cooling,” International Journal of Heat and Mass Transfer, 17(5), pp 595-607.

[13] Schmidt, D. L., and Sen, B., 1996, “Film Cooling with Compound Angle Holes: Adiabatic Effectiveness,” Journal of Turbomachinery, 118(4), pp 807-813.

[14] Sen, B., Schmidt, D. L., and Bogard, D. G., 1996, “Film Cooling with Compound Angle Holes: Heat Transfer,” ASME Journal of Turbomachinery

[15] Taslim, M. E., and Khanicheh, A., 2005, “Film Effectiveness Downstream of a Row of compound Angle Film Holes,” Journal of Heat Transfer, 127

[16] Baldauf, S., Schulz, A., and Wittig, S., 2001, “High-Resolution Measurements of Local Effectiveness from Discrete Hole Film Cooling,” Journal of Turbomachinery-Transactions of the ASME, 123(4), pp 758-765

[17] Yuen, C. H. N., and Martinez-Botas, R., 2005, “Film Cooling Characteristics of Rows of Round Holes at various Streamwise Angles in a Crossflow: Part I. Effectiveness,” International Journal of Heat and Mass Transfer, 48(23-24), pp 4995-5016

[18] Ekkad, S. V., Zapata, D., and Han, J. C., 1997, “Film Effectiveness over a Flat Surface with Air and CO_2 Injection through Compound Angle Holes using a Transient Liquid Crystal Image Method,” ASME Journal of Turbomachinery, 119, pp 587-593

[19] Liqrani, P. M., and Sik Lee, J., 1996, “Film Cooling from a Single Row of Compound Angle Holes at High Blowing Ratios,” International Journal of Rotating Machinery, 2(4), pp 259-267

[20] Nasir, H., Ekkad, S. V., and Acharya, S., 2001, “Effect of Compound Angle Injection on Flat Surface Film Cooling with Large Streamwise Injection Angle,” Experimental Thermal and Fluid Science, 25(23)

[21] Aga, V., 2011, “Influence of Flow Structure on Compound Angled Film Cooling Effectiveness and Heat Transfer,” Journal of Turbomachinery, 133(3)

[22] Ligrani, P. M., Wigle, J. M., Ciriello, S., and Jackson, S. M., 1994, “Film Cooling from Holes with Compound Angle Orientations: Part 1—Results Downstream of Two Staggered Rows of Holes with 3d Spanwise Spacing,” ASME Journal of Heat Transfer, 116(2)

[23] Maiteh, B. Y., and Jubran, B. A., 2004, “Effects of Pressure Gradient on Film Cooling Effectiveness from Two Rows of Simple and Compound Angle Holes in Combination,” Energy Conversion and Management, 45, pp 1457-1469

[24] Jubran, B. A., and Maiteh, B. Y., 1999, “Film Cooling and Heat transfer from a Combination of Two rows of Simple and/or Compound Angle Holes in Inline and/or Staggered Configuration,” Heat and Mass Transfer, 34, pp 495-502

[25] Kusterer, K., Bohn, D., Sugimoto, T., and Tanaka, R., 2007, “Double-Jet Ejection of Cooling Air for Improved Film Cooling,” ASME Journal of Turbomachinery, 129(4), pp 809-815

[26] Heidmann, J., and Ekkad, S., 2007, “A Novel Anti-Vortex Turbine Film Cooling Hole Concept,” ASME Paper GT2007- 27528.

[27] Dhungel, A., Lu, Y., Philips, A., Ekkad, S., and Heidmann, J., 2007, “Film Cooling from a Row of Holes Supplemented with Anti Vortex Holes,” ASME Gas Turbine Conference, ASME Paper, GT2007-27419

[28] Leblanc, C., Narzary, D., and Ekkad, S. V., 2007, “Film Cooling Performance of an Anti-Vortex Hole on a Flat Plate,” AJTEC, Hawaii. (AJTEC2011-44161)

[29] Ekkad, S. V., and Han, J. C., 2013, “A Review of Hole Geometry and Coolant Density Effect on Film Cooling,” Proceedings of the 2013 Summer Heat Transfer Conference, Minnesota, Paper no. HT2013-17250

[30] Yang, W., Liu, X., Li, G., and Zhang, J., 2012, “Experimental Investigation on Heat Transfer Characteristics of Film Cooling using Parallel-Inlet Holes,” International Journal of Thermal Sciences, 60, pp 32-40

[31] Baldauf, S., Scheurlen, M., Schulz, A., and Wittig, S., 2002, “Correlation of Film-Cooling Effectiveness from Thermographic Measurements at Engine like Conditions,” Journal of Turbomachinery, 124, pp 686-698

[32] Han, J. C., and Mehendale, A. B., 1986, “Flat-Plate Film Cooling with Steam Injection through One row and Two rows of Inclined Holes,” Journal of Turbomachinery, 108, pp 137-144

[33] Jubran, B., and Brown, A., 1985, “Film Cooling from Two rows of Holes Inclined in the Streamwise and Spanwise Directions,” ASME Journal of Engineering for Gas Turbines and Power, 107(1), pp 84-89

[34] Jubran, B. A., Al-Hamadi, A., and Theodoridis, G., 1997, “Film Cooling and Heat Transfer with Air Injection through Two Rows of Compound Angle Holes,” Heat and Mass Transfer, 33(1-2), pp 93-100

[35] Mayle, P., 1975, “Multihole Cooling Film Effectiveness and Heat transfer,” ASME Heat Transfer Divison, Paper no. 74- HT-9

[36] Burd, S. W., Kaszeta, R. W., and Simon, T. W., 1998, “Measurements in Film Cooling Flows: Hole L/D and Turbulence Intensity Effects,” Journal of Turbomachinery, 120(4), pp 791-798

[37] Lutum, J., 1999, “Influence of the Hole Length-to-Diameter Ratio on Film Cooling with Cylindrical Holes,” Journal of Turbomachinery, 121(2), pp 209-216

[38] Gritsch, M., Colban, W., Schar, H., and Dobbeling, K., 2005, “Effect of Hole Geometry on the Thermal Performance of Fan-Shaped Film Cooling Holes,” Journal of Turbomachinery-Transactions of the ASME, 127(4), pp 718-725

[39] Pedersen, D., Eckert, E., and Goldstein, R., 1977, “Film Cooling with Large Density Differences between the Mainstream and the Secondary Fluid measured by the Heat Mass Transfer Analogy,” ASME Transactions Journal of Heat Transfer, 99, pp 620-627

[40] Sinha, A. K., Bogard, D., and Crawford, M., 1991, “Film Cooling Effectiveness Downstream of a Single Row of Holes with Variable Density Ratio,” Journal of Turbomachinery, 113(3), pp 442-449

[41] Wright, L. M., Gao, Z., Varvel, T. A., and Han, J. C., 2005, “Assessment of Steady State PSP, TSP, and IR Measurement Techniques for Flat Plate Film Cooling,” Proceedings of ASME Turbo Expo, ASME paper no. HT2005-72363

[42] Chen, A., Li, S. J., and Han, J. C., 2014, “Film Cooling with Forward and Backward Injection for Cylindrical and Fan Shaped Holes using PSP Measurement Technique,” Proceedings of ASME Turbo Expo 2014: Turbine Technical Conference and Exposition GT2014, Vancouver, Canada

[43] Young, C. D., Rivir, R. B., Han, J. C., and Huang, Y. Y., 1992, “Influence of Jet-Grid Turbulence on Flat plate Turbulent Boundary Layer Flow and Heat Transfer,” Journal of Heat Transfer, 114, pp 65-72

[44] Wright, L. M., McClain, S. T., and Clemenson, M. D., 2011, “Effect of Density Ratio on Flat Plate Film Cooling with Shaped Holes using PSP,” Journal of Turbomachinery, 133(4)

[45] Kline, S. J., and Mcclintock, F. A., 1953, “Describing Uncertainties in a Single Sample Experiment,” Mechanical Engineering (ASME), 75, pp 3-8

APPENDIX

Contours and average effectiveness plots for all cases are given in the following pages.

Test matrix and figure title is given in table below.

Plate #	Row 1	Row 2	Row 3	Parameters		Figure Number
	β	β	β	Arrangement	p/d	-
A	45	45	45	In line	4	A1-A2
B	45	45	45	Row 2 & 3 staggered	4	B1-B2
C	45	-45	-45	In line	4	C1-C2
D	45	-45	-45	Row 2 & 3 staggered	4	D1-D2
E	45	45	45	In line	6	E1-E2
F	45	45	45	Row 2 & 3 staggered	6	F1-F2
G	45	-45	-45	In line	6	G1-G2
H	45	-45	-45	Row 2 & 3 staggered	6	H1-H2
I	45	45	45	In line	8	I1-I2
J	45	45	45	Row 2 & 3 staggered	8	J1-J2
K	45	-45	-45	In line	8	K1-K2
L	45	-45	-45	Row 2 & 3 staggered	8	L1-L2

List of additional comparison plots comparing different designs are presented as under:

Figure a	Average effectiveness plot - effect of hole angle and arrangement for varying M at DR 1
Figure b	Average effectiveness plot - effect of hole angle and arrangement for varying M at DR 1.5
Figure c	Average effectiveness plot - effect of hole angle and arrangement for varying M at DR 2.0
Figure d	Effect of p/d on average effectiveness (Plate A) for different M and DR
Figure e	Effect of p/d on average effectiveness (Plate D) for different M and DR

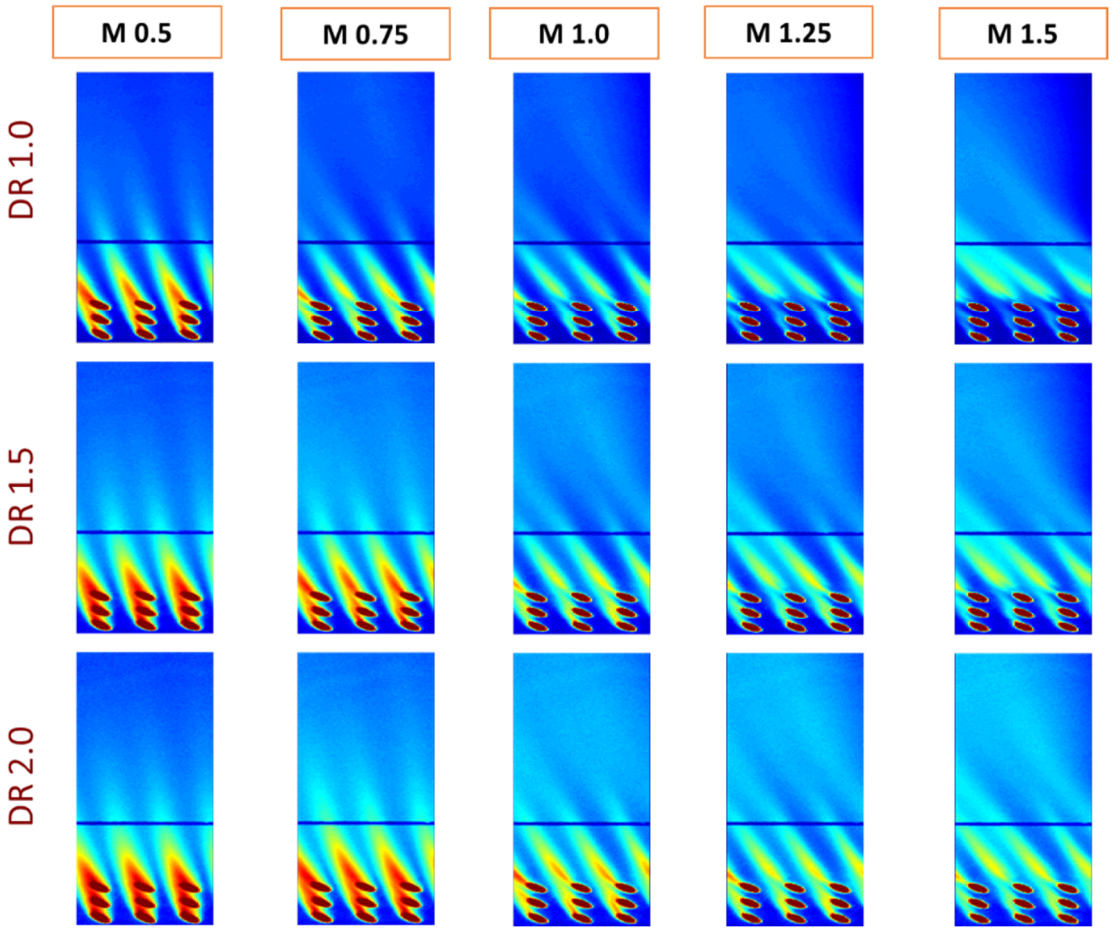

Figure A1: Effectiveness contour for Plate A for different density ratios and blowing ratios

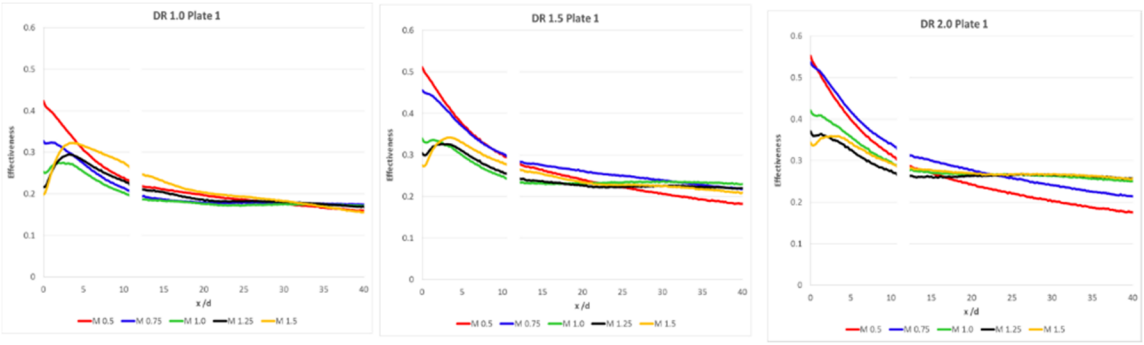

Figure A2: Effectiveness plots for Plate A for different density ratios and blowing ratios

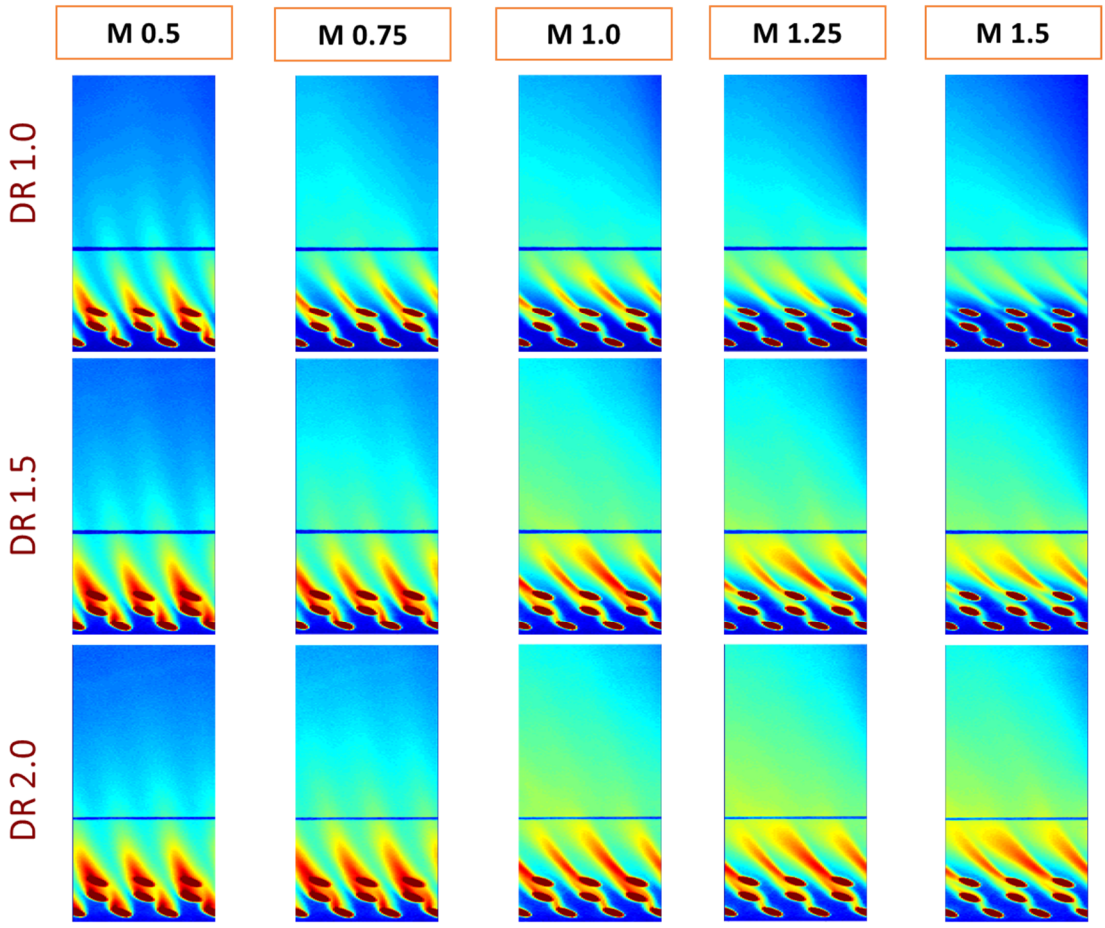

Figure B1: Effectiveness contour for Plate B for different density ratios and blowing ratios

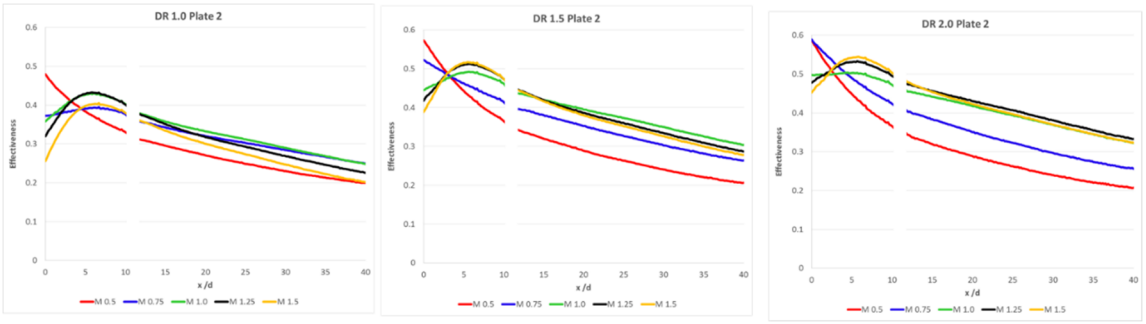

Figure B2: Effectiveness plots for Plate B for different density ratios and blowing ratios

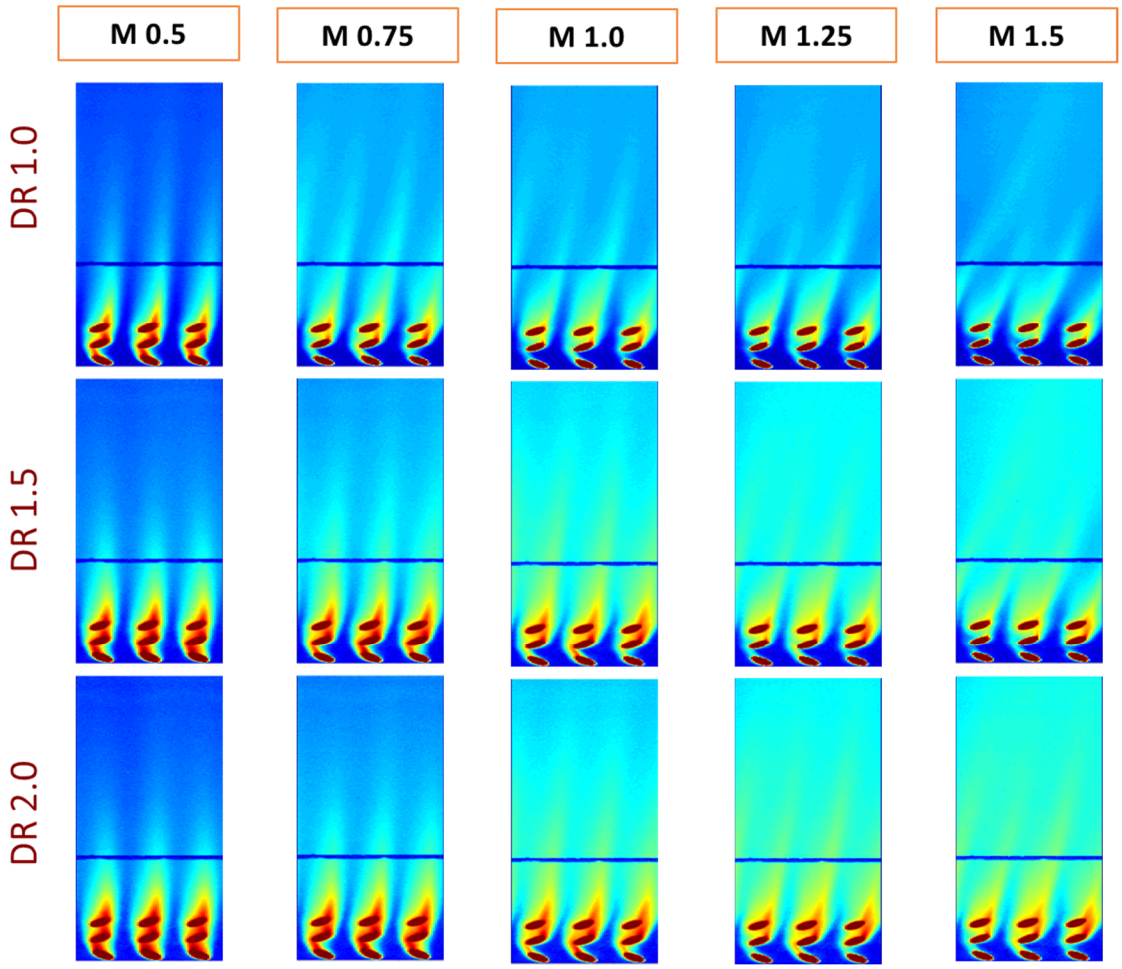

Figure C1: Effectiveness contour for Plate C for different density ratios and blowing ratio

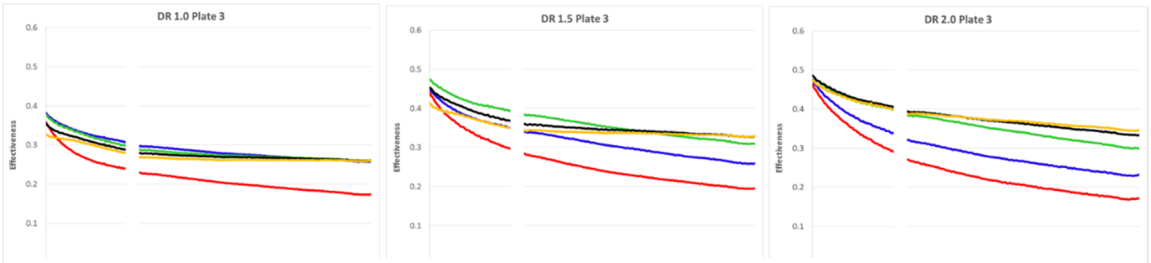

Figure C2: Effectiveness plots for Plate C for different density ratios and blowing ratios

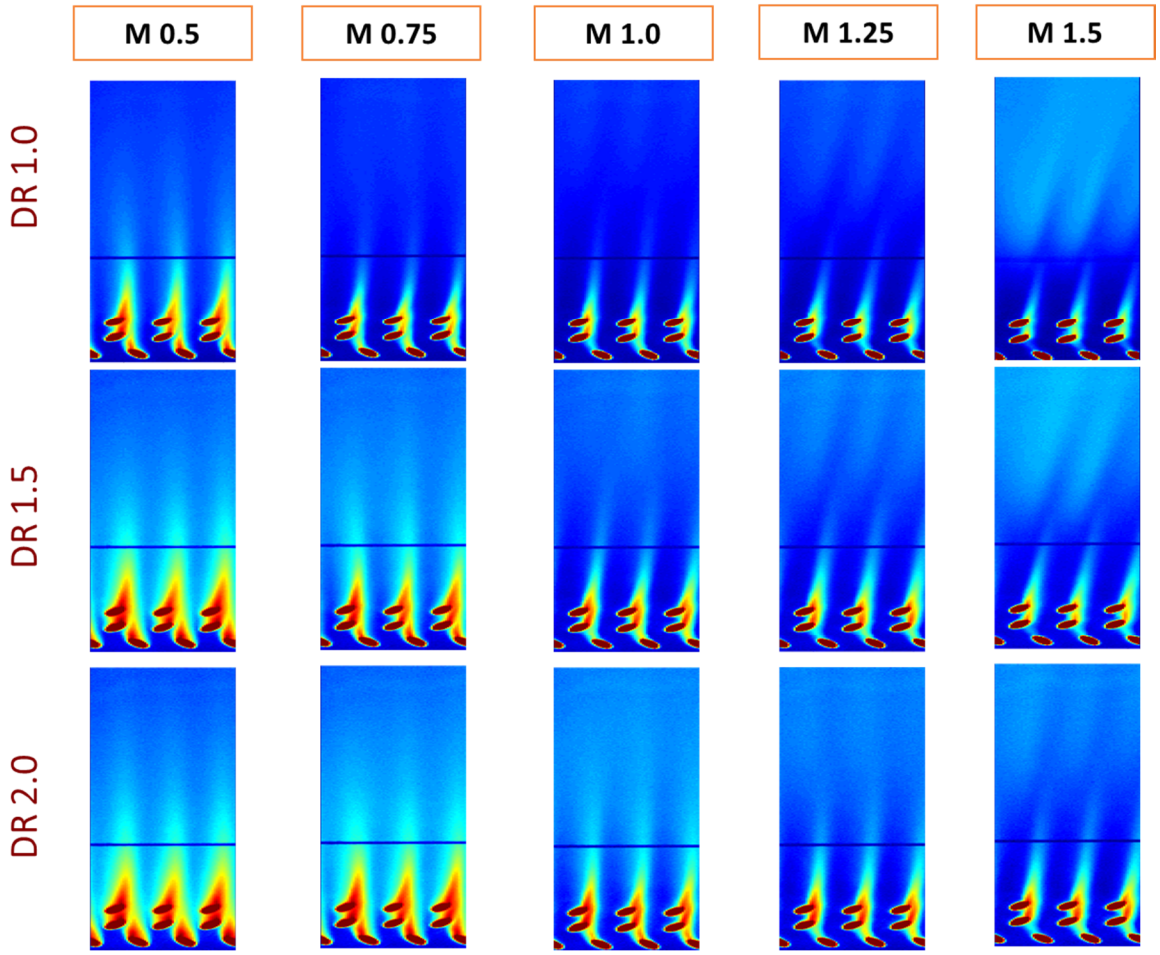

Figure D1: Effectiveness contour for Plate D for different density ratios and blowing ratios

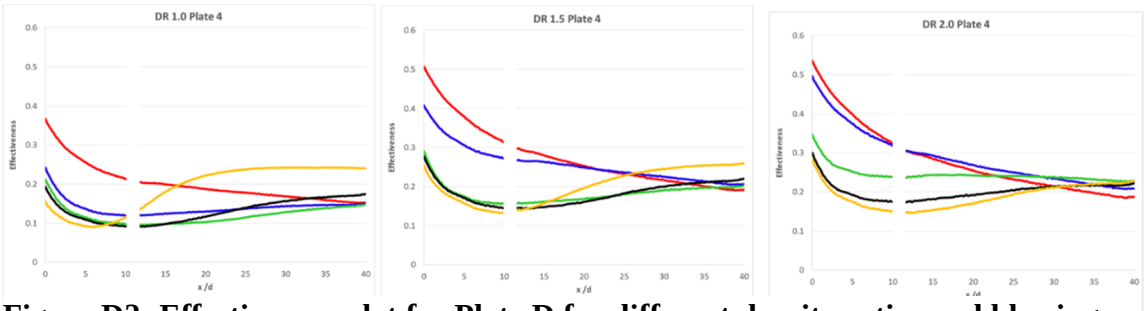

Figure D2: Effectiveness plot for Plate D for different density ratios and blowing ratios

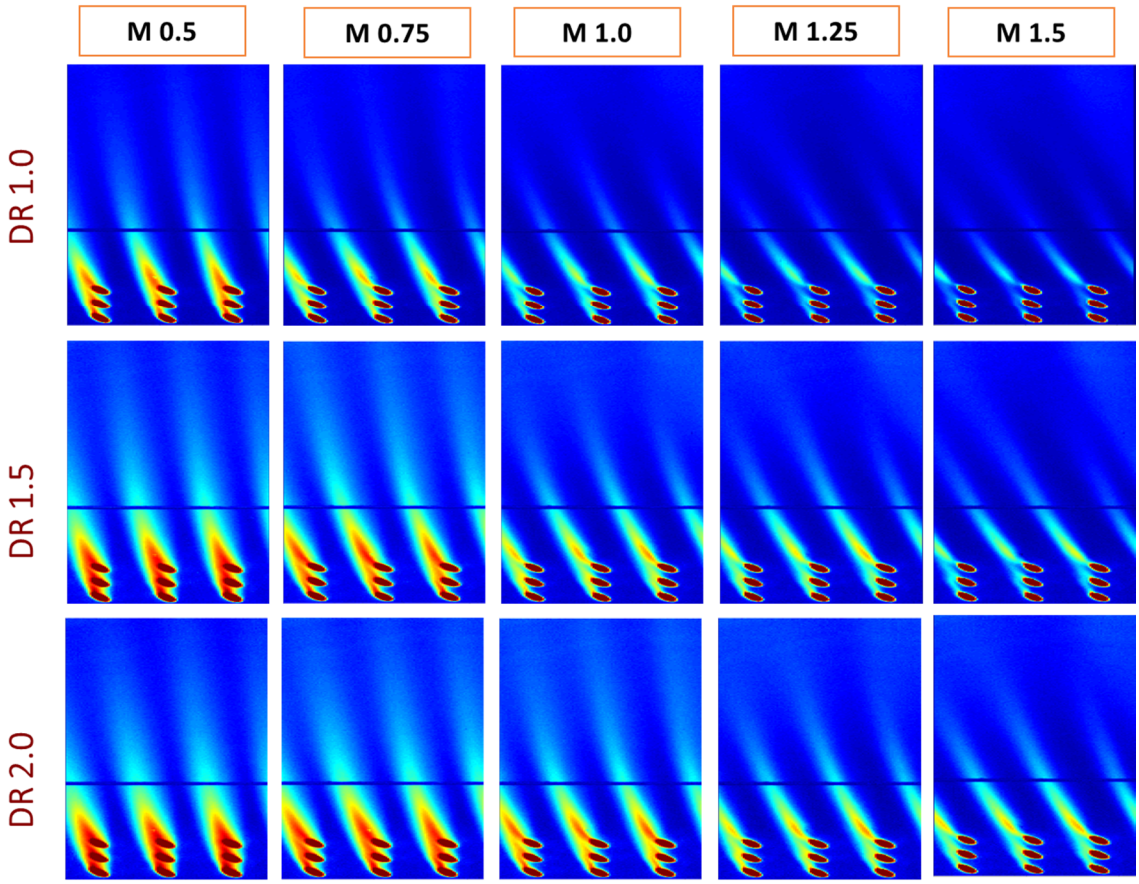

Figure E1: Effectiveness contour for Plate E for different density ratios and blowing ratios

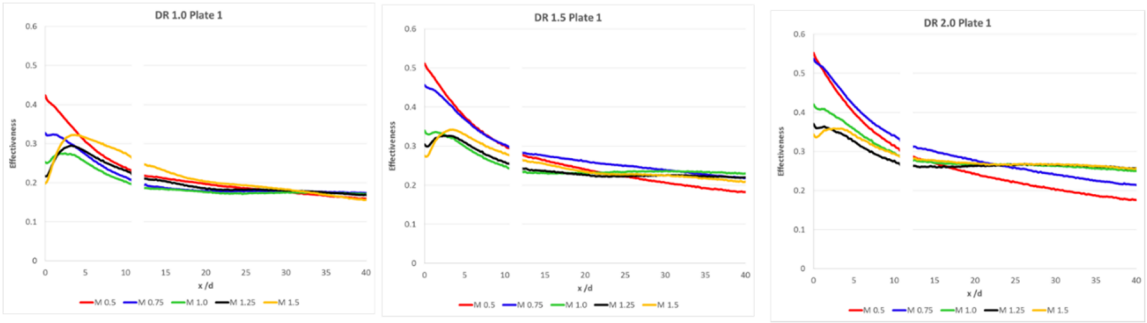

Figure E2: Effectiveness plot for Plate E for different density ratios and blowing ratios

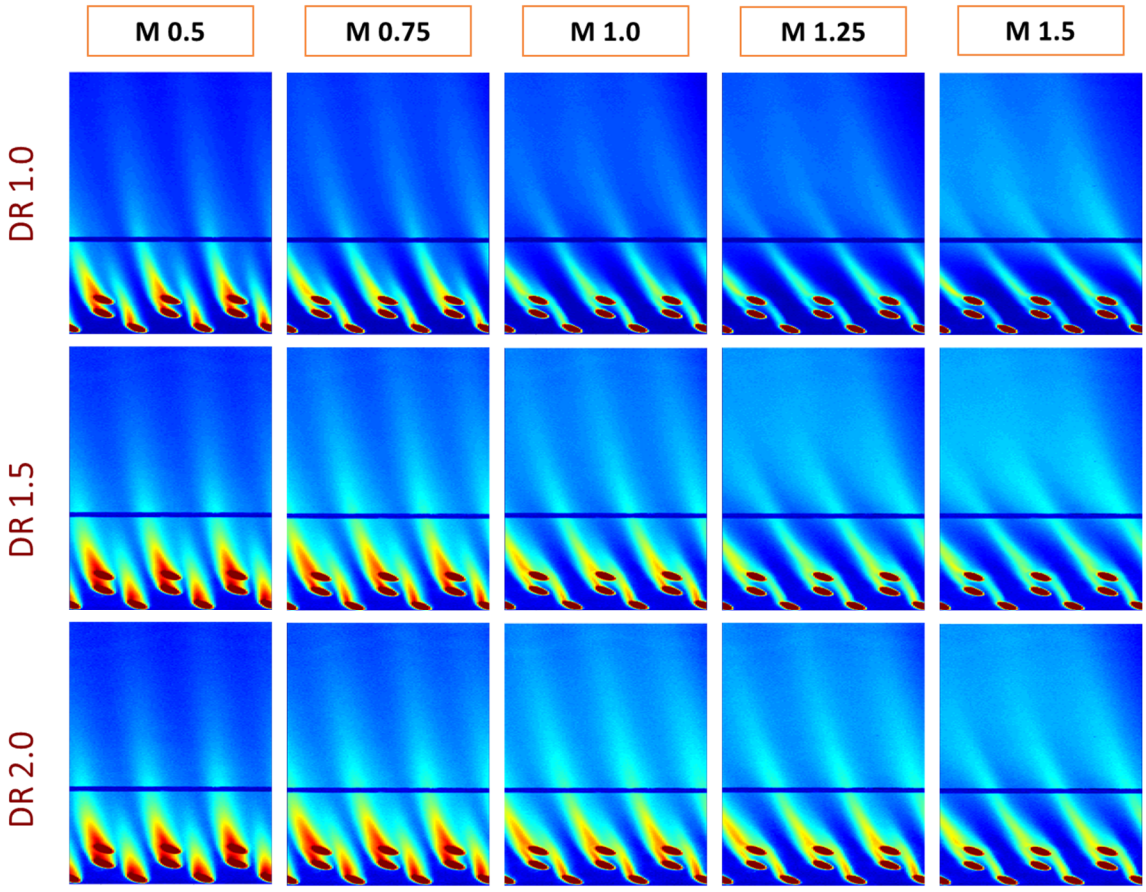

Figure F1: Effectiveness plot for Plate F for different density ratios and blowing ratios

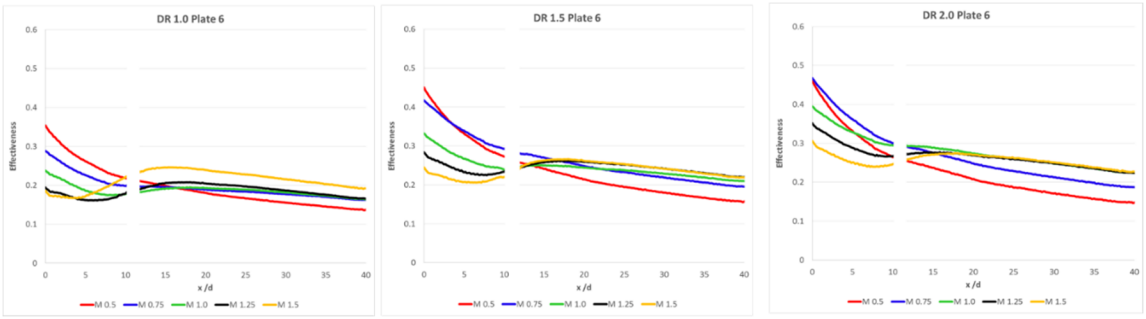

Figure F2: Effectiveness plot for Plate F for different density ratios and blowing ratios

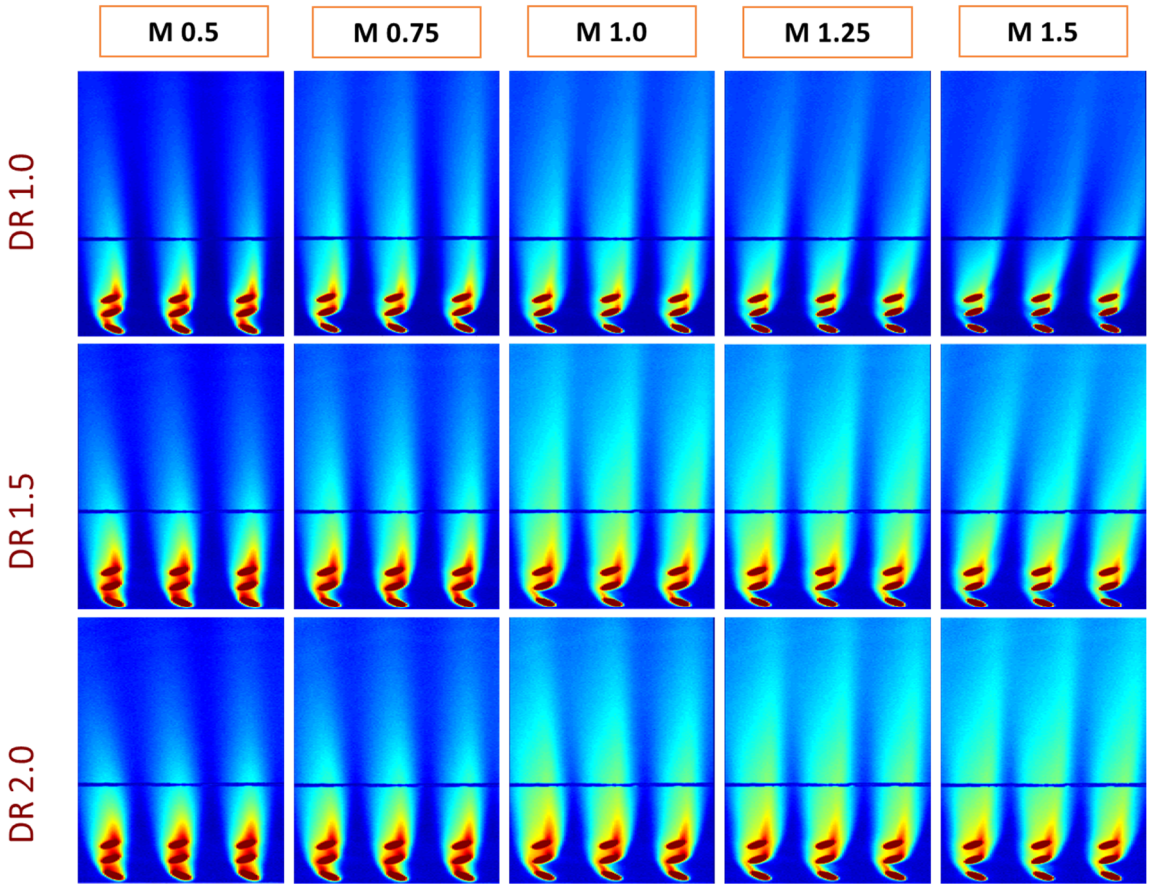

Figure G1: Effectiveness contour for Plate G for different density ratios and blowing ratios

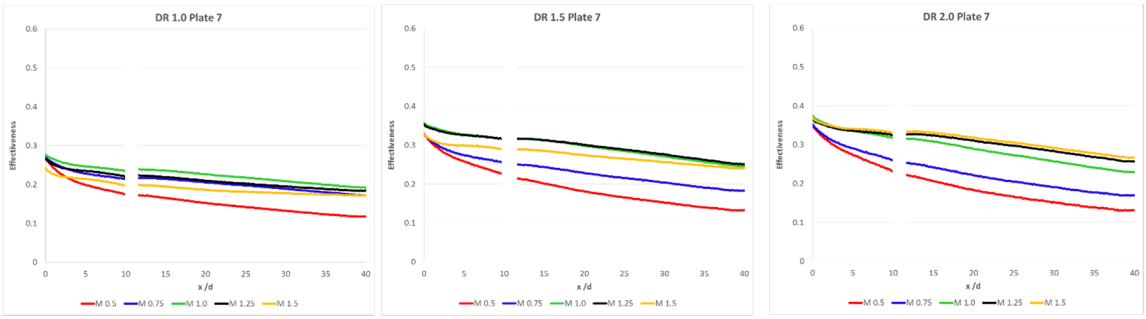

Figure G2: Effectiveness plot for Plate G for different density ratios and blowing ratios

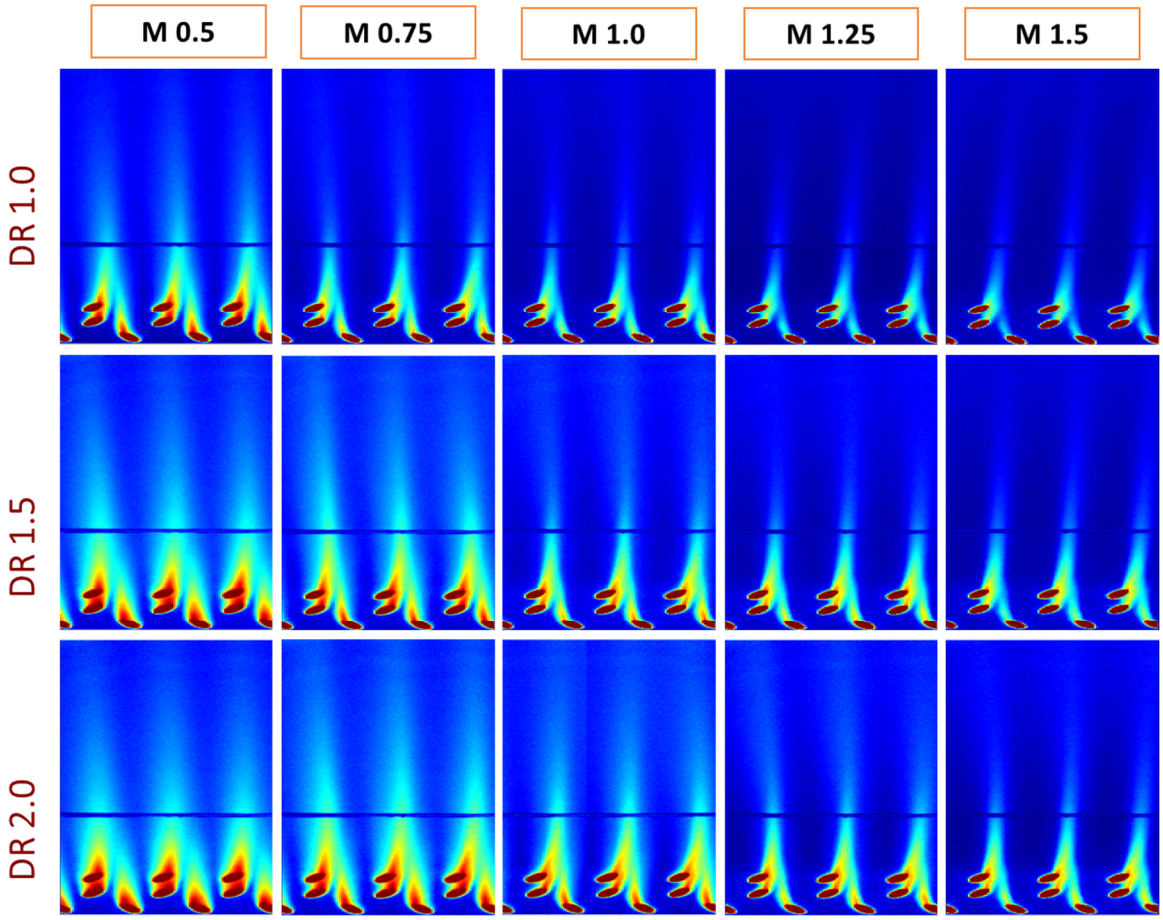

Figure H1: Effectiveness contour for Plate H for different density ratios and blowing ratios

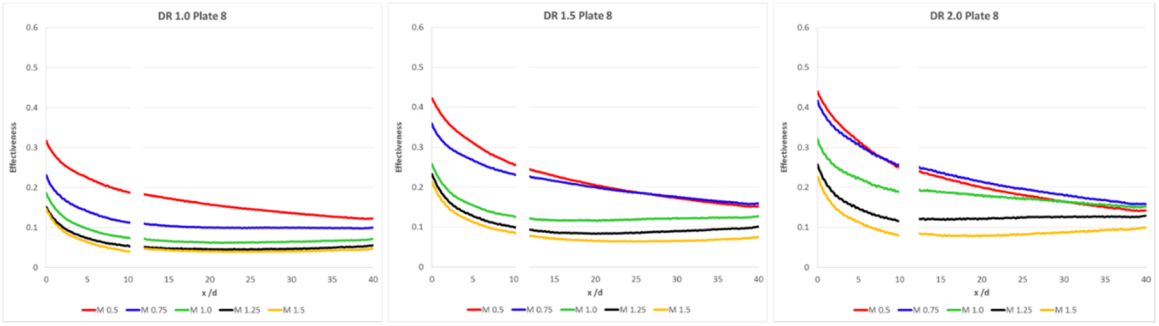

Figure H2: Effectiveness plot for Plate H for different density ratios and blowing ratios

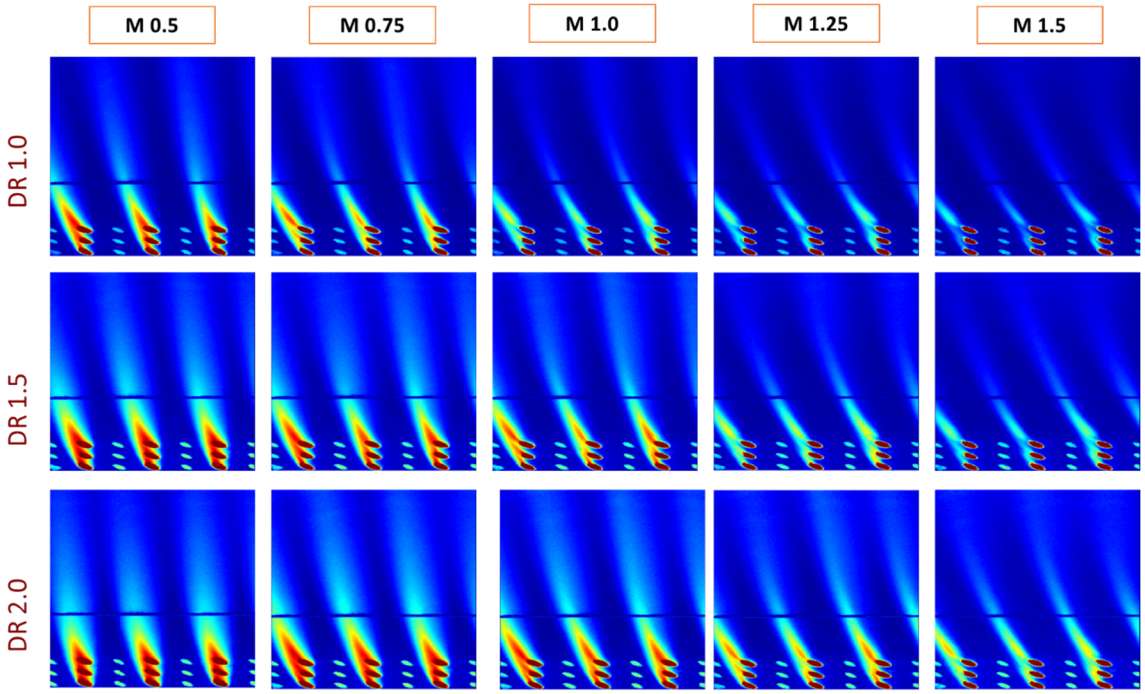

Figure I1: Effectiveness contour for Plate I for different density ratios and blowing

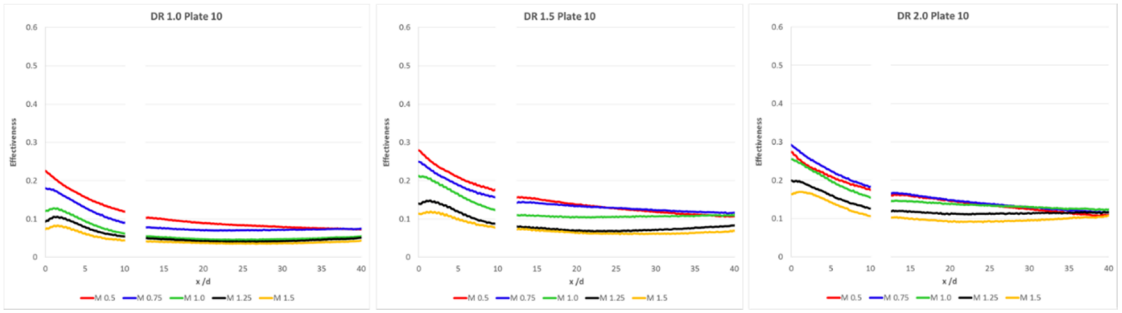

Figure I2: Effectiveness plot for Plate I for different density ratios and blowing

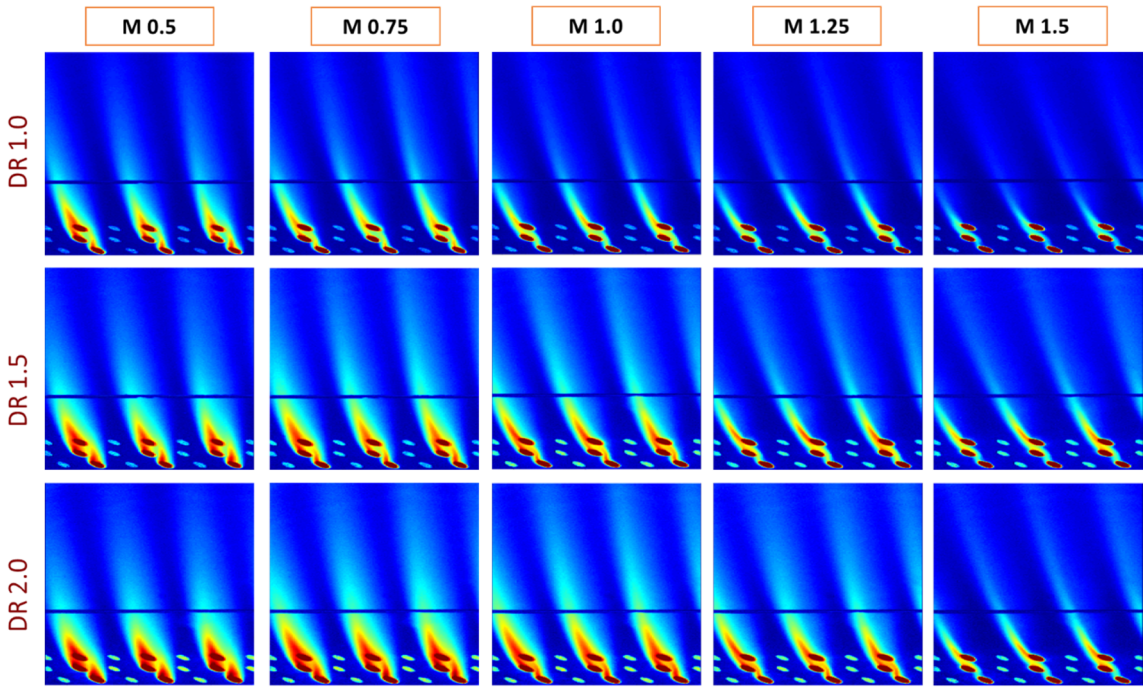

Figure J1: Effectiveness contour for Plate J for different density ratios and blowing ratios

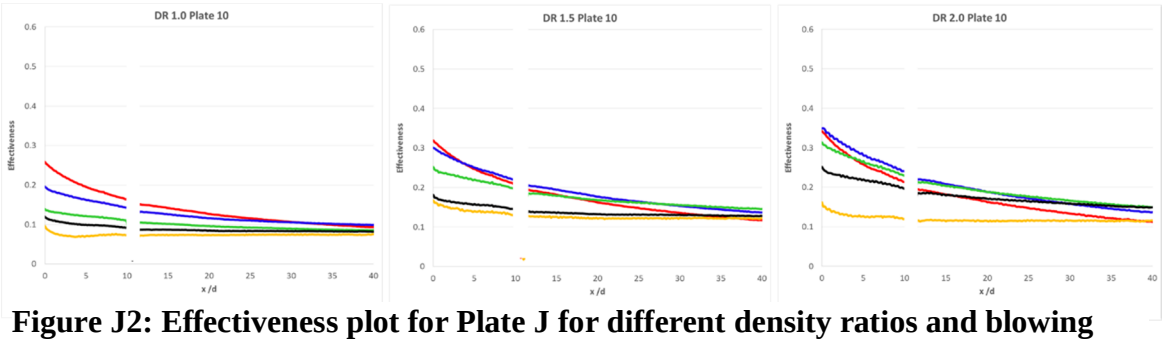

Figure J2: Effectiveness plot for Plate J for different density ratios and blowing ratios

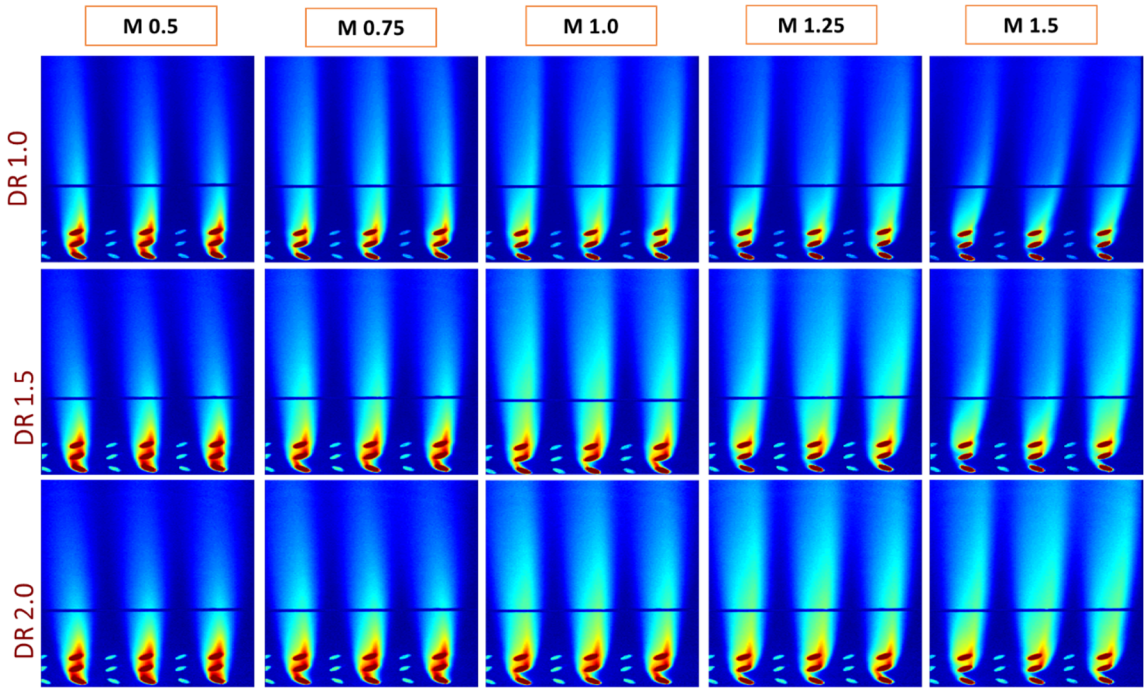

Figure K1: Effectiveness contour for Plate K for different density ratios and blowing ratio

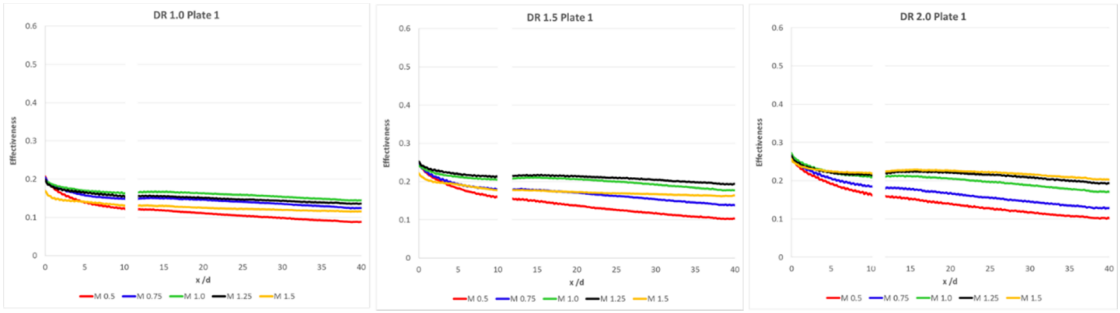

Figure K2: Effectiveness plot for Plate K for different density ratios and blowing ratios

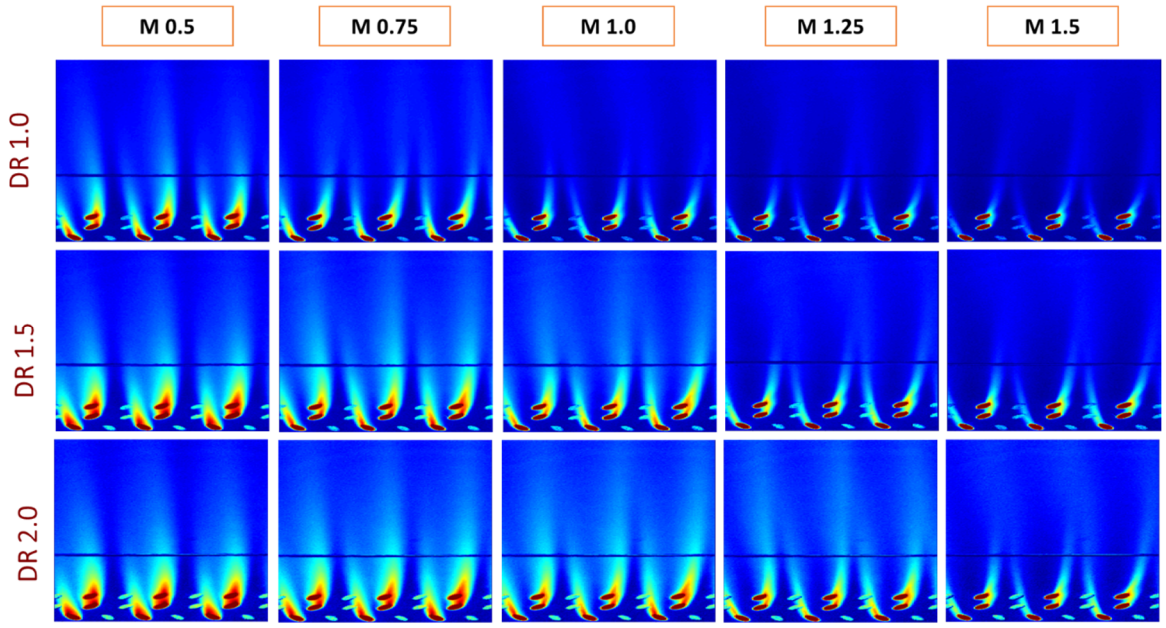

Figure L1: Effectiveness contour for Plate L for different density ratios and blowing

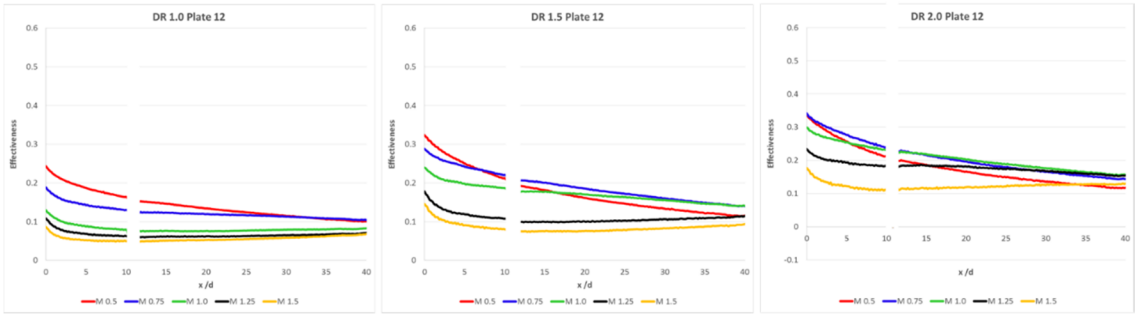

Figure L2: Effectiveness plot for Plate L for different density ratios and blowing ratios

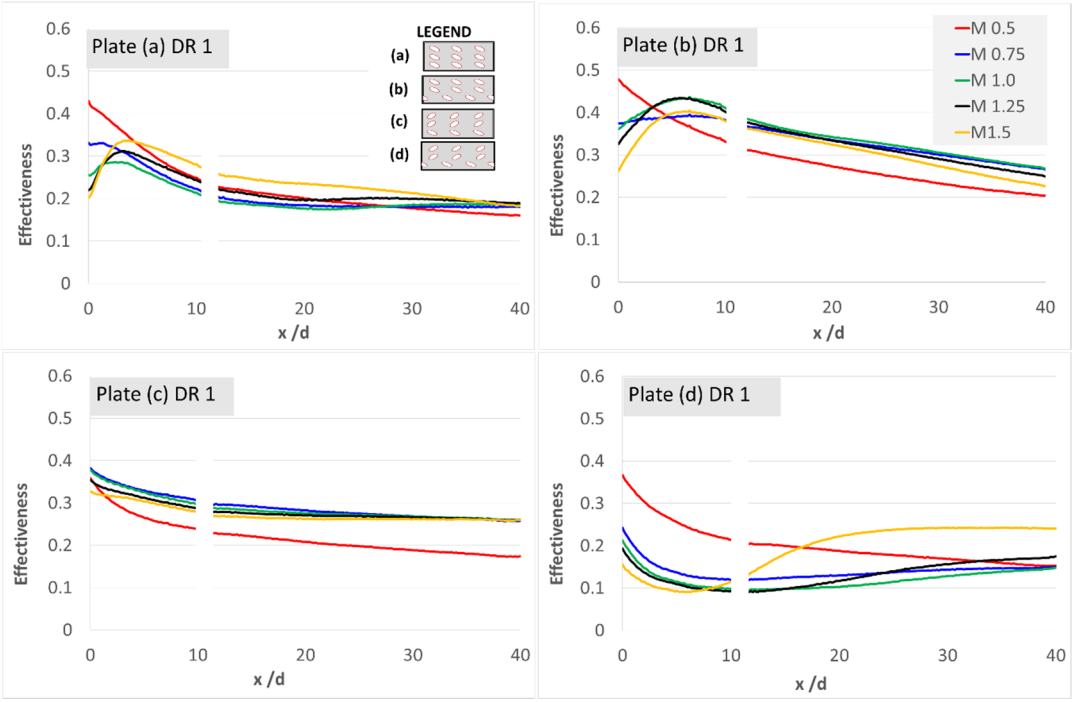

Figure a: Average effectiveness plot - effect of hole angle and arrangement for varying M at DR 1

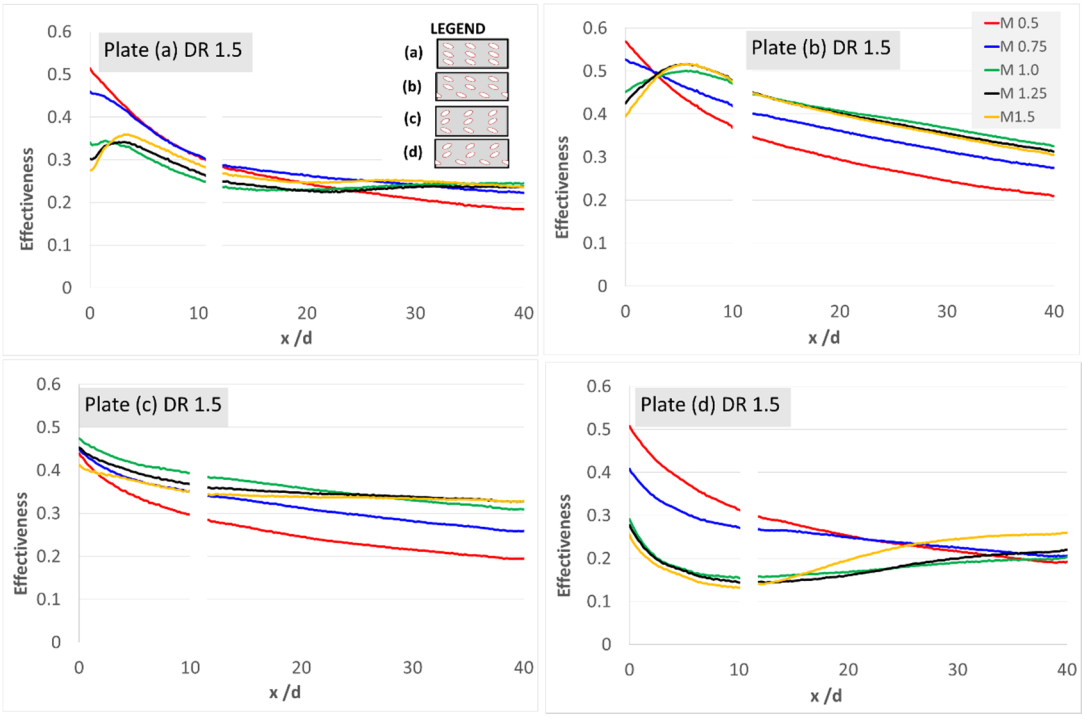

Figure b: Average effectiveness plot - effect of hole angle and arrangement for varying M at DR 1.5

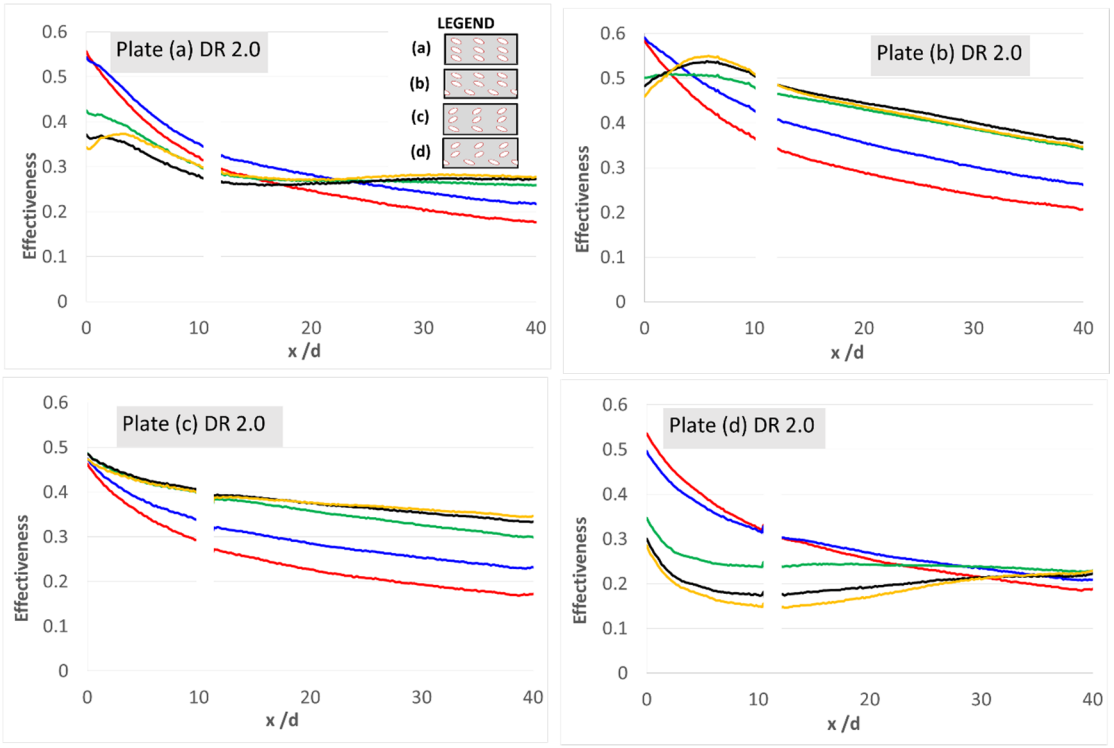

Figure c: Average effectiveness plot - effect of hole angle and arrangement for varying M at DR 2.0

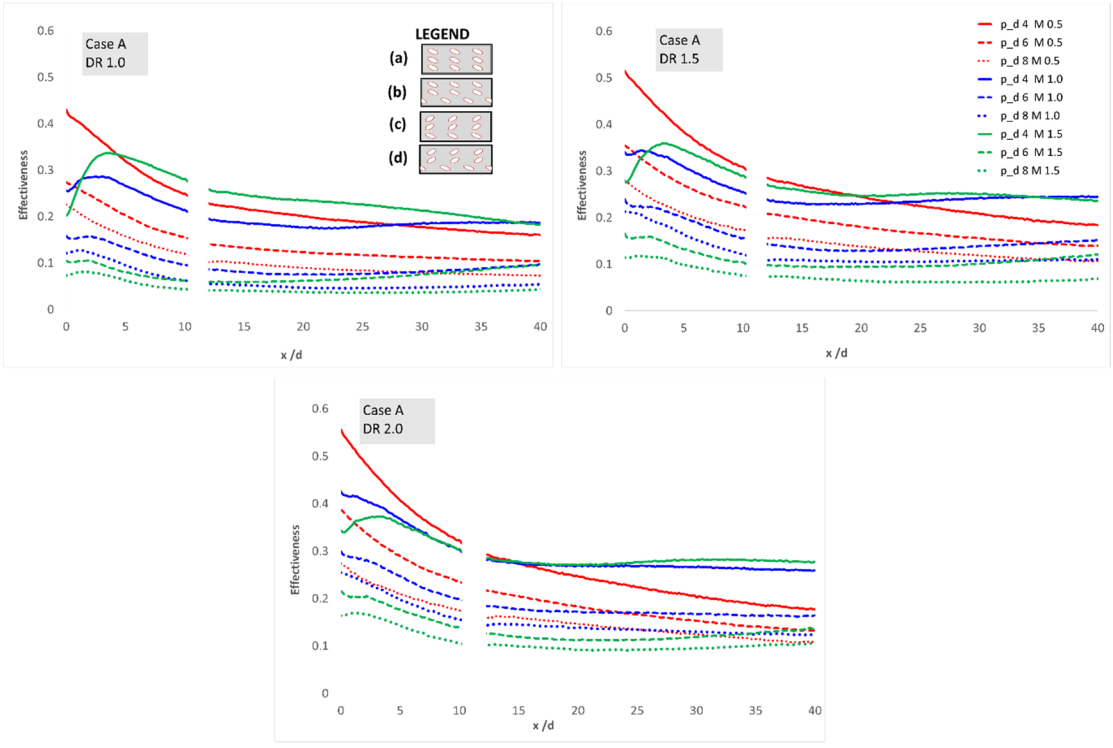

Figure d: Effect of p/d on average effectiveness (Plate A) for different M and DR

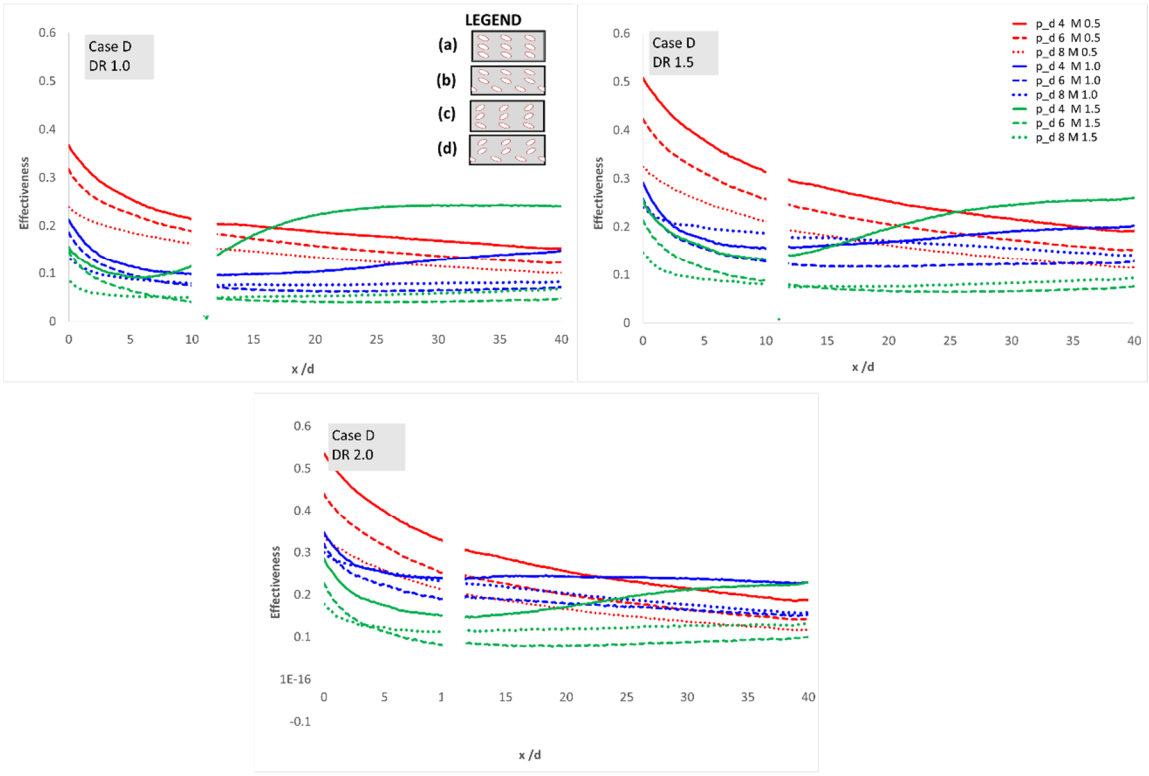

Figure e: Effect of p/d on average effectiveness (Plate D) for different M and DR